New Phytologist

Tansley review

Evaluating theories of drought-induced vegetation mortality using a multimodel–experiment framework

Author for correspondence
Nate G. McDowell
Tel:+1 505 665 2909
Email: mcdowell@lanl.gov

Received: *5 June 2013*
Accepted: *19 July 2013*

Nate G. McDowell[1], Rosie A. Fisher[2], Chonggang Xu[1], J. C. Domec[3,4], Teemu Hölttä[5], D. Scott Mackay[6], John S. Sperry[7], Amanda Boutz[8], Lee Dickman[1], Nathan Gehres[8], Jean Marc Limousin[8], Alison Macalady[9], Jordi Martínez-Vilalta[10,11], Maurizio Mencuccini[12,13], Jennifer A. Plaut[8], Jérôme Ogée[14], Robert E. Pangle[8], Daniel P. Rasse[15], Michael G. Ryan[16,17], Sanna Sevanto[1], Richard H. Waring[18], A. Park Williams[1], Enrico A. Yepez[19] and William T. Pockman[8]

[1]Earth and Environmental Sciences Division, Los Alamos National Laboratory, Los Alamos, NM 87545, USA; [2]Climate and Global Dynamics Division, National Center for Atmospheric Research, Boulder, CO 80305, USA; [3]University of Bordeaux, Bordeaux Sciences Agro, UMR INRA-TCEM 1220, 33140 Villenave d'Ornon, France; [4]Nicholas School of the Environment, Duke University, Box 90328, Durham, NC 27708, USA; [5]Department of Forest Sciences, University of Helsinki, PO Box 24, 00014, Helsinki, Finland; [6]Department of Geography, State University of New York at Buffalo, 105 Wilkeson Quadrangle, Buffalo, NY 14261, USA; [7]Department of Biology, University of Utah, 257 South 1400 East, Salt Lake City, UT 84112, USA; [8]Department of Biology, MSC03 2020, 1 University of New Mexico, Albuquerque, NM 87131-0001, USA; [9]School of Geography and Development and Laboratory of Tree-Ring Research, University of Arizona, 1215 Lowell Street, Tucson, AZ 85721-0058, USA; [10]CREAF, Cerdanyola del Vallès, 08193, Spain; [11]Univ Autònoma Barcelona, Cerdanyola del Vallès 08193, Spain; [12]ICREA at CREAF, Cerdanyola del Vallès 08193, Spain; [13]School of GeoSciences, University of Edinburgh Crew Building, West Mains Road, Edinburgh, EH9 3JN, UK; [14]INRA, UR1263 EPHYSE, F-33140, Villenave d'Ornon, France; [15]Bioforsk – Norwegian Institute for Agricultural and Environmental Research, Ås, Norway; [16]Natural Resource Ecology Laboratory, Colorado State University, Fort Collins, CO 80523-1499, USA; [17]USDA Forest Service, Rocky Mountain Research Station, Fort Collins, CO 80526, USA; [18]College of Forestry, Oregon State University, Corvallis, OR 97331-5704, USA; [19]Departamento de Ciencias del Agua y del Medio Ambiente, Instituto Tecnológico de Sonora, Ciudad Obregón, Sonora, 85000, Mexico

Contents

New Phytologist (2013) **200:** 304–321
doi: 10.1111/nph.12465

Key words: carbon starvation, cavitation, die-off, dynamic global vegetation models (DGVMs), hydraulic failure, photosynthesis, process-based models.

Summary

Model–data comparisons of plant physiological processes provide an understanding of mechanisms underlying vegetation responses to climate. We simulated the physiology of a piñon pine–juniper woodland (*Pinus edulis–Juniperus monosperma*) that experienced mortality during a 5 yr precipitation-reduction experiment, allowing a framework with which to examine our knowledge of drought-induced tree mortality. We used six models designed for scales ranging from individual plants to a global level, all containing state-of-the-art representations of the internal hydraulic and carbohydrate dynamics of woody plants. Despite the large range of model structures, tuning, and parameterization employed, all simulations predicted hydraulic failure and carbon starvation processes co-occurring in dying trees of both species, with the time spent with severe hydraulic failure and carbon starvation, rather than absolute thresholds *per se*, being a better predictor of impending mortality. Model and empirical data suggest that limited carbon and water exchanges at stomatal, phloem, and below-ground interfaces were associated with mortality of both species. The model–data comparison suggests that the introduction of a mechanistic process into physiology-based models provides equal or improved predictive power over traditional process-model or empirical thresholds. Both biophysical and empirical modeling approaches are useful in understanding processes, particularly when the models fail, because they reveal mechanisms that are likely to underlie mortality. We suggest that for some ecosystems, integration of mechanistic pathogen models into current vegetation models, and evaluation against observations, could result in a breakthrough capability to simulate vegetation dynamics.

I. Background

Accelerating rates of vegetation mortality in association with drought and rising temperature have now been documented in all major global biomes (van Mantgem *et al.*, 2009; Allen *et al.*, 2010; Phillips *et al.*, 2010; Beck *et al.*, 2011; Carnicer *et al.*, 2011; Peng *et al.*, 2011; Liu *et al.*, 2013; Williams *et al.*, 2013). Mortality is expected to increase as a result of rising temperature and increasing drought frequency and severity (Breshears *et al.*, 2005; Allison *et al.*, 2009; Lewis *et al.*, 2011; Dietze & Moorcroft, 2012; Williams *et al.*, 2013), with large biogeochemical and biophysical climatic feedbacks expected to follow as a result of shifts in land carbon and energy balance (Bonan, 2008; Kurz *et al.*, 2008).

A primary motivation for examining our understanding of drought-induced mortality is the large international demand for realistic land surface modeling to enable accurate climate projections (Bonan, 2008; Allison *et al.*, 2009; Arora *et al.*, 2013). Mortality of widespread plant functional types (PFTs) within models has a large impact on the prediction of terrestrial climate forcing and future climate in dynamic global vegetation models (DGVMs; Hurtt *et al.*, 1998; Sitch *et al.*, 2003; Friedlingstein *et al.*, 2006; Purves & Pacala, 2008; Allison *et al.*, 2009). The mortality algorithms within most DGVMs are relatively simple and represent neither the current understanding of how PFTs die during drought nor the internal status of carbon and water in vegetation under drought stress (Moorcroft, 2006; McDowell *et al.*, 2011). The current limits to mechanistic mortality modeling are driven in part by the lack of direct experimental tests of mortality theory (McDowell & Sevanto, 2010) and evaluation against data. Forecasts of future mortality can also be extrapolated from historic, empirical relationships (e.g. Williams *et al.*, 2013). Thus, we need to determine not only the dominant mechanisms driving mortality for fundamental understanding, but also the degree of empirical vs theoretical prediction that is required to accurately simulate mortality, ideally using a common evaluation framework (e.g. Luo *et al.*, 2012).

In the current absence of a community benchmark effort for model predictions of mortality, an alternative and more immediate option is to examine our model-based understanding within the constraints of ecosystem drought manipulations (e.g. Galbraith *et al.*, 2010; Powell *et al.*, 2013). Multi-model evaluations thus far have revealed that accurate simulation of traditional fluxes (e.g., photosynthesis and transpiration) does not equate to accurate prediction of mortality, partly as a result of both hydraulic and carbon metabolism uncertainties during severe drought (Galbraith *et al.*, 2010; Powell *et al.*, 2013). Our study complements these through a similar model–experiment framework, but with a focus on the mechanisms of mortality.

There are multiple inclusive hypotheses regarding the underlying drivers of drought-induced mortality: hydraulic failure, or desiccation as a result of cessation of water transport; carbon starvation, or the lethal impairment of metabolism or failure to defend against biotic attack as a result of depletion of carbohydrate stores; and an interdependency of carbon starvation, hydraulic failure, and biotic attack (summarized in McDowell *et al.*, 2011; Fig. 1). Failure to maintain a sufficient phloem turgor gradient to drive carbohydrate flow from sources to sinks can hasten mortality through carbon starvation (Sala *et al.*, 2010) or hydraulic failure (McDowell *et al.*, 2011) or both (Sevanto *et al.*, 2013). Novel glasshouse and field observations have clearly demonstrated the importance of both carbon starvation and hydraulic failure in mortality (Adams *et al.*, 2009; Breshears *et al.*, 2009; Anderegg *et al.*, 2012; Plaut *et al.*, 2012; Hartmann *et al.*, 2013; Quirk *et al.*, 2013; Sevanto *et al.*, 2013).

Theories on drought-induced plant mortality scale biophysical and ecological principles (Waring, 1987; McDowell *et al.*, 2008;

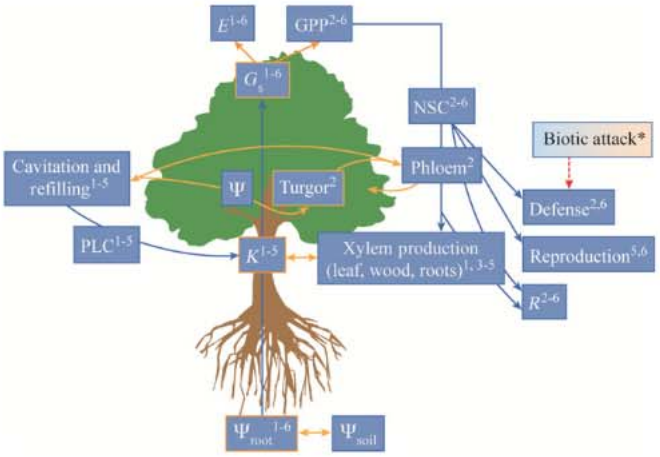

Fig. 1 A generalized simulation scheme for modeling plant hydraulic failure, carbon starvation, and their interdependence. The numbers within each box indicate inclusion by the following models: 1, Sperry model; 2, FINNSIM; 3, TREES; 4, MuSICA; 5, ED(X); 6 CLM(ED). Orange-bordered boxes and orange arrows indicate interdependencies, or bidirectional carbon water fluxes, that are simulated by the models. Allocation of nonstructural carbohydrate (NSC) to defense, reproduction, respiration, and growth is not listed in priority order, because that remains a subject of debate. *E*, canopy transpiration; G_s, canopy-scale stomatal conductance; *K*, hydraulic conductance; PLC, percentage loss of conductance; Ψ_{soil} and Ψ_{root}, soil and root water potential; GPP, gross primary production; *R*, autotrophic respiration. *Biotic attack was not included in any of the models used in this study, but is included to highlight the need for this critical model development (red arrow). Feedbacks between biotic attack and plant physiology are not highlighted here.

Raffa *et al.*, 2008), including numerous water–carbon feedbacks (e.g. McDowell *et al.*, 2011), making hypothesis testing challenging even with manipulative experiments. The original, groundbreaking models of internal hydraulic or carbohydrate dynamics (Thornley, 1972; Tyree & Sperry, 1988; Amthor & McCree, 1990) have been recently developed across plant (Sperry *et al.*, 1998; Hölttä *et al.*, 2006, 2009; Rasse & Tocquin, 2006), ecosystem (Williams *et al.*, 2001; Mackay *et al.*, 2003; Domec *et al.*, 2012), and global scales (Hickler *et al.*, 2006; Fisher *et al.*, 2010). These types of models synthesize our understanding of the complex hydraulic-carbohydrate system of vegetation (e.g. Cowan & Troughton, 1971; McDowell, 2011) and can thus be employed to investigate complex, dynamical processes such as drought responses of forests (e.g. Williams *et al.*, 2001).

We used a model–experiment approach as a framework to examine our collective knowledge regarding how trees survive and die during drought. We began with reviewing and clarifying the definitions of hydraulic failure and carbon starvation that represent our state-of-knowledge of plant mortality and are simultaneously compatible with the current framework of most process models and DGVMs. We then drove six models using input parameters from a replicated drought manipulation study in a mature piñon pine–juniper woodland (*Pinus edulis–Juniperus monosperma*) in central New Mexico, USA. It has been predicted through both a DGVM and an empirical model that the southwestern USA will experience almost 100% mortality of the dominant conifers by 2050 (Jiang *et al.*, 2013; Williams *et al.*, 2013). The models employed here represent individual plant-scale (two models), ecosystem-scale (two models), and two global-scale DGVMs. Models were employed to simulate either or both hydraulic failure and carbon starvation and their interdependencies. Additionally, the mortality predictions from the carbon starvation algorithms in the two DGVMs were compared with observations, traditional process-model mortality indices, and an empirical tree-ring model.

II. Model–experiment approach

1. Overall approach

Our objective was to examine our model-based understanding of drought-induced mortality. We simulated the response of pine and juniper trees to experimental drought (Plaut *et al.*, 2012, 2013; Gaylord *et al.*, 2013; Limousin *et al.*, 2013) as a way of capturing the complex and often unmeasurable internal hydraulic and carbohydrate dynamics. Specifically, we examined multimodel simulations of the mechanistic processes of hydraulic failure, carbon starvation, and their interdependency, as well as more traditional simulations of mortality using net primary production (NPP), growth efficiency (NPP yr^{-1} per leaf area), and an empirical model based on regional tree-ring datasets (Williams *et al.*, 2013). We compared simulations with observations of transpiration (*E*) for evaluation, and additional parameters depending on the model. We did not make predictions about the future nor did we conduct formal comparisons of the models, because three of them lacked replicate simulations (their smallest scale was the plot scale). We identified consistencies and discrepancies across models and empirical observations.

We employed models that varied in structure and scale, from individual plants to a global level, in the approximate following order: FINNSIM (Hölttä *et al.*, 2006, 2009), the Sperry model (Sperry *et al.*, 1998), TREES (Loranty *et al.*, 2012; Mackay *et al.*, 2012), MuSICA (Ogée *et al.*, 2003; Domec *et al.*, 2012), ED(X) (Fisher *et al.*, 2010; Xu *et al.*, 2012), and CLM(ED) (Fisher *et al.*, 2010; Bonan *et al.*, 2012). The unique, common characteristic of the models used here is the ability to simulate internal plant hydraulics and/or carbon dynamics (Fig. 1). These capabilities are novel in woody plant, ecosystem, and global-scale modeling, and allow predictions of processes consistent with the postulated proximate drivers of plant death.

2. Definitions of hydraulic failure, carbon starvation, their interdependence, and mortality

We defined the process of hydraulic failure as the progressive loss of hydraulic conductivity (*K*) on an individual-plant basis (Fig. 1). The loss of *K* for all models was scaled and reported as the percentage loss of conductance (PLC; 0–100%). The advantages of PLC as a definition of hydraulic failure are that it is quantitative, measurable, scalable to PFTs, and it inherently accepts that static PLC-mortality thresholds do not exist (e.g. Sevanto *et al.*, 2013). This definition assumes that conductance–vulnerability curves on soils, roots, and branches scale to whole-tree *K*. This definition

further assumes that PLC < 100% impacts the function of downstream foliage (e.g. Hubbard *et al.*, 2001). Hydraulic failure has been previously defined at the distal tissue level as 100% PLC (Sperry *et al.*, 1998; Davis *et al.*, 2002), and at the whole-plant level as the PLC that results in insufficient hydration to maintain metabolism (McDowell *et al.*, 2008, 2011). Defining hydraulic failure of the PLC continuum assumes that PLC < 100% may be sufficient to jeopardize water balance and metabolic function; analogous to metabolic impacts of a chronic > 50% reduction in mammalian cardiovascular circulation.

We defined the process of carbon starvation as the depletion of available nonstructural carbohydrates (NSC; Fig. 1). The advantages and assumptions of this definition are similar to those for PLC. Carbon starvation has been previously defined as prolonged zero photosynthesis (Martínez-Vilalta *et al.*, 2002; Ward *et al.*, 2005; McDowell *et al.*, 2008), as strictly 100% NSC loss (Sala *et al.*, 2010), and as the loss of carbohydrates available for maintenance of defense, metabolism, and turgor (McDowell, 2011; McDowell *et al.*, 2011). Like PLC, the continuum definition of carbon starvation is quantitative and logical because partial NSC loss may be sufficient to lethally impair metabolism, defense, and turgor (McDowell, 2011; Hoch *et al.*, 2003; Gruber *et al.*, 2012; Richardson *et al.*, 2013).

Interdependence of hydraulic failure and carbon starvation is defined as increasing PLC and associated xylem tensions causing declining carbon uptake, transport, or utilization, and subsequent feedbacks by which declining available NSC impacts PLC through refilling or water acquisition (modified from McDowell *et al.*, 2011). No models simulated biotic attack in this study (Fig. 1), but the interdependence definition should ideally include water and carbon feedbacks on defense and subsequent biotic agent population dynamics.

Mortality was quantified in the field as the percentage loss of foliated crown and was measured annually (Gaylord *et al.*, 2013). When piñon pine dies in association with bark beetle (*Ips* spp.) attack (as occurred in two of the three drought plots in 2008), the entire canopy progresses from green to orange (zero water content) in *c.* 4 wk (Breshears *et al.*, 2009; Plaut *et al.*, 2012; Gaylord *et al.*, 2013). Juniper, by contrast, drops individual twigs and branches as drought progresses, maintaining individual survival for longer than pine but progressively losing leaf area (Gaylord *et al.*, 2013). Trees were pronounced dead at 0% foliated canopy.

We defined mortality in the two DGVMs, ED(X) and CLM (ED), as a threshold minimum carbohydrate content per unit leaf area. Only ED(X) and CLM(ED) have explicit mortality predictions; the other models simulated physiological processes but did not have thresholds or triggers for mortality. Mortality predictions from these models have not previously been tested.

3. Modeling PLC and NSC

Loss of xylem conductivity with decreasing xylem water potential was represented using Weibull functions fit to PLC and water potential (□) data for species- and site-specific measurements (see Plaut *et al.*, 2012, and Supporting Information, Notes S1, Fig. S1)

$$PLC = 100\left(1 - e^{-\left(\frac{\psi}{b}\right)^{c}}\right) \quad \text{Eqn 1}$$

where ψ values are branch and root water potential values (MPa), b is the critical □ that leads to 63% of conductivity reduction and c is a shape parameter (Sperry & Tyree, 1988; Pammenter & Van der Willigen, 1998). The Weibull function was the best fit to the vulnerability curve data (Plaut *et al.*, 2012; and Notes S1, Fig. S1). These vulnerability curves are measured on branches and roots, allowing tissue-specific calculation of PLC from □ measurements or estimates. PLC is both theoretically and practically useful for investigating hydraulic failure, and has the additional value of broad coverage of plant functional types in the literature (e.g. Maherali *et al.*, 2004; Choat *et al.*, 2012), thus enabling input into future DGVM simulations.

While our models shared Eqn 1 for simulating PLC, they differed in their treatment of below-ground hydraulics and stomatal regulation (Tables 1, S1). Sperry, TREES, MuSICA, and CLM(ED) had multiple depths of root water uptake and explicit soil–root hydraulic conductance, whereas ED(X) simulated a single soil water pool. ED(X) assumed soil □ equaled root □, whereas the smaller-scale models prevented root □ from falling below the midday observed □. FINNSIM used root □ simulated by MuSICA. All models (except FINNSIM) assumed xylem refilling followed the species- and tissue-specific vulnerability curves (Eqn 1, Notes S1). In Sperry and TREES, the soil was assumed to immediately recover hydraulic conductance on rewetting, but not the xylem. Xylem refilling (or recovery via new xylem growth) was indicated when fluxes were underpredicted post-drought, and the models were recalibrated accordingly.

Modeling approaches for NSC are less well tested than for PLC because of our poor understanding of NSC storage in trees (Le Roux *et al.*, 2001; McDowell & Sevanto, 2010; Sala *et al.*, 2012; Richardson *et al.*, 2013). Many models do not include a storage pool, and, for those that do, the controls on fluxes in and out of the storage pool are poorly constrained. Theoretical and empirical evidence suggests that over the lifetime of plants, allocation to storage is probably an equal priority to growth (Waring & Schlesinger, 1985; Chapin *et al.*, 1990; Hoch *et al.*, 2003; Rasse & Tocquin, 2006; Smith & Stitt, 2007; Sulpice *et al.*, 2009; McDowell, 2011; Sala *et al.*, 2012; Stitt & Zeeman, 2012; Wiley & Helliker, 2012). In our study, the models that simulated NSC (TREES, MuSICA, ED(X) and CLM(ED)) used various modifications to the general NSC overflow approach that included feedbacks to prevent growth or respiration from consuming all NSC (Table 1; similar to Rasse & Tocquin, 2006), which is consistent with evidence from many studies (reviewed in McDowell, 2011; Sala *et al.*, 2012; Stitt & Zeeman, 2012), including extreme tests of carbon starvation via 100% shading (e.g. Marshall & Waring, 1985; Sevanto *et al.*, 2013). TREES, MuSICA, and ED (X) decreased growth as carbohydrate storage declined, and CLM (ED) effectively did the same by lowering tissue turnover rate and homeostatically increasing storage fluxes as carbohydrate storage declined.

Table 1 Key processes in mortality simulation

Model/scale	G_s control	C-H_2O points of interaction[a]	Internal water and carbon status	GPP and *R* regulation in drought	Partitioning rules
FINNSIM Plant	*E* is given as input	Phloem turgor; C cost of cavitation refilling	Cavitation frees H_2O proportional to PLC Sugar-starch dynamics via Michaelis–Menten kinetics. Phloem transport distributes NSC	GPP and *R* are given as input	N/A
Sperry Plant	Darcy's law	N/A	Steady state N/A	N/A	Root : shoot *K* = 1 : 1
TREES Plant/ ecosystem	Darcy's law, VPD	g_s–*A*; no refilling if NSC is zero; growth and *R* decline with K; root uptake	Steady state for this analysis Initial NSC proportional to biomass; withdrawn for *R* first, then growth	Both are down-regulated	Maintenance *R* first, NSC storage, root/shoot growth last
MuSICA Ecosystem	Ball–Berry–Tardieu–Davies	g_s–*A*; root uptake	Water capacitance scales with leaf area; *K* with fine root length; hydraulic redistribution Single NSC pool; source kinetics	Both down-regulated except maintenance *R*	N/A (biomass prescribed in current simulations)
ED(X) Ecosystem/global	Ball-Berry	g_s–*A* regulated via *K*; root uptake	Vulnerability curves, soil □ drive PLC Single NSC pool, storage determined by equilibrium concentration ratios of tissues. Pool size driven by GPP, respiration, and the carbon sink rate depending on the target storage	Maximum carboxylation and maintenance *R* reduced 50% if NSC is < 8% leaf biomass	Storage followed by maintenance *R*, turnover, and then growth
CLM(ED) Ecosystem/global	Ball–Berry	Root uptake	Single NSC pool regulated to approach target level; declines if GPP-*R* turnover is negative	GPP reduced with moisture stress. No reduction of *R*	Maintenance *R* followed by turnover, growth then storage

G_s, canopy conductance; *E*, evapotranspiration; PLC, percentage loss of conductance; NSC, nonstructural carbohydrates; GPP, gross primary production; *R*, respiration (maintenance unless indicated otherwise); *K*, hydraulic conductivity. ED(X) and CLM(ED) induce mortality at NSC < 8% and 10% of leaf biomass, respectively. The other models lack mortality rules

[a]The stomatal (*E*–GPP), xylem–phloem, and H_2O uptake/root carbon allocation interfaces (e.g. Fig. 1). N/A, not applicable.

Interactions between phloem function and xylem refilling (Zwieniecki & Holbrook, 2009; Secchi & Zwieniecki, 2012) were mechanistically investigated using a new, coupled xylem–phloem transport model FINNSIM (based on Hölttä *et al.*, 2006, 2009). FINNSIM used the gross primary production (GPP) and growth from MuSICA plus scaled respiration estimates (see Notes S2a) to estimate fluxes among the NSC pool, phloem, and xylem. This was the only model to examine theoretical carbon costs of xylem refilling, but because it was run with MuSICA simulations for input, it was excluded from ensemble analyses.

ED(X) and CLM(ED) represent a class of DGVMs that simulate the biogeochemistry, biophysics, and demographics of global plant functional types (Cox *et al.*, 1998; Moorcroft *et al.*, 2001; Woodward & Lomas, 2004; Sitch *et al.*, 2008; Medvigy *et al.*, 2009; Fisher *et al.*, 2010; Oleson *et al.*, 2010; Zaehle *et al.*, 2010; Medvigy & Moorcroft, 2012). DGVM mortality predictions have not performed well in tropical drought manipulation studies (Galbraith *et al.*, 2010; Powell *et al.*, 2013); ours is the first test in the temperate zone.

ED(X) and CLM(ED) are aggregated models and thus could not simulate individual trees, but rather simulated cohorts of average trees within each functional type, size, and demographic status (Moorcroft *et al.*, 2001). Because these models simulated the entire drought and ambient plots, there are no replicates of these simulations and thus intermodel comparisons are not statistically possible. All the models used tree allometric equations (Notes S2a) for the root, stem and leaf structural carbon pools and measured leaf NSC (Notes S2b) at the site for initiating the carbon pools. To accommodate different model requirements for stand, soil or physiological inputs, we distributed all available data from the precipitation–manipulation experiment to each modeler (see Table S1 for variables). The data used for calibration and evaluation varied for the different models, but all models used *E* for a common evaluation. Additional model details can be found in the Notes S3.

4. Field experiment

The study site is located within the Sevilleta National Wildlife Refuge, New Mexico (34°23′11″ N, 106°31′46″ W). The site is a piñon pine (*Pinus edulis* Englm.) and juniper (*Juniperus monosperma* Englm. (Sarg.)) savannah (Romme *et al.*, 2009). These sympatric species are excellent models of drought responses because of their contrasting hydraulic strategies (McDowell *et al.*, 2008). Piñon pine is relatively isohydric, maintaining midday leaf □ within a narrow range despite large treatment and seasonal variations in soil □ (Plaut *et al.*, 2012). The pine's stomatal closure during drought reduces photosynthesis (Limousin *et al.*, 2013). Juniper is relatively anisohydric, allowing greater photosynthesis during drought by maintaining higher stomatal conductance and tolerating lower leaf □ (Plaut *et al.*, 2012; Limousin *et al.*, 2013). Piñon pine is more vulnerable to drought than juniper (Breshears *et al.*, 2005; Plaut *et al.*, 2012), but has relatively similar midday □, vulnerability curves, and other physiological traits similar to most members of the *Pinaceae* (Maherali *et al.*, 2004; Choat *et al.*, 2012). Juniper is representative of cavitation-resistant species in seasonally dry regions (Maherali *et al.*, 2004; Choat *et al.*, 2012).

The field site is located in the lower latitudinal and elevational ranges of both species (Romme *et al.*, 2009). The climate, physical setting, and study design are described in detail elsewhere (Pangle *et al.*, 2012; Plaut *et al.*, 2012; Limousin *et al.*, 2013). Briefly, mean annual temperature and precipitation are 12.7°C (SE 0.13) and 363 mm (SE 21.5), respectively (20 yr record), with a bimodal distribution of precipitation, with peaks in the winter and late summer (monsoon), and with a pronounced dry period during the spring and early summer. The experiment consists of three 40 m × 40 m (1600 m^2) replicate plots of four treatments: water addition by overhead sprinklers; 45% precipitation removal using gutters ('drought'); an infrastructure control with inverted gutters allowing 100% of ambient subcanopy precipitation to reach the soil; and ambient control. The plots were blocked based on aspect, and treatments were imposed in August 2007 (Pangle *et al.*, 2012).

Simulations of one drought and one ambient plot (or individual trees within plots, depending on model) are considered to represent simulations of trees that died and those that survived, respectively, because of the large amount of mortality in the drought plot. The models used input data from the southeast-facing drought and control plots to simulate individual trees or groups of trees. This block was selected because it had the longest-running data, and a large amount of mortality occurred on this block (and on the north-facing block; Gaylord *et al.*, 2013). Piñon pine in the drought plot exhibited 68% mortality by December 2008 (Plaut *et al.*, 2012; Gaylord *et al.*, 2013) and 100% mortality by May 2009 in association with beetle attack. Juniper trees exhibited limited canopy dieback in 2008, but by 2011, 30% of the mature trees had < 15% green canopy remaining and one mature juniper was completely dead (for a total of 60% canopy loss by 2011, Gaylord *et al.*, 2013). No trees died on the ambient plot. All models were run only for these two plots.

Models were parameterized with data from January 2007 to December 2010, including near-monthly measurements of pre-dawn □, daily mean soil □, half-hourly or daily *E* (beginning in April 2007), half-hourly meteorological data (solar radiation, air and soil temperature, and precipitation) as well as standard metrics of stand density, tree diameter and height, biomass, leaf area, soil depth, texture, and nutrient content. Meteorological data were collected at midcanopy height. Soil temperature was measured at 5 cm depth and □$_s$ was measured at 15 and 20 cm depths to ensure similar measurement depths across all soil profiles despite variation in depth to bedrock. In addition, leaf and stem samples were collected throughout the study and analyzed for NSC (Notes S2b). A list of variables used by the models is provided in Table S1.

5. Evaluation of *E* simulations

Models were parameterized and evaluated individually against multiple datasets, but all models shared calibration using species-specific, sapflow-based *E* (per unit sapwood area to avoid scaling issues) measured in spring 2007 when the drought infrastructure had not yet been installed and seasonal drought had not yet initiated (Plaut *et al.*, 2012). Likewise, all models were evaluated against *E* observations from August 2007 (the date of drought structure installation) to 2010 at least. *E* is the

longest, most continuous, and potentially the most relevant observation in this study (Plaut *et al.*, 2013), because it integrates whole-plant hydraulics and carbon uptake, and E is also a common output variable of most process models. Note that FINNSIM did not simulate E but utilized MuSICA's simulations as input.

Comparison of observed and simulated E demonstrates an example of the challenge of evaluating DGVMs, which are designed for regional to global application, at single sites. These large-scale models have fewer mechanisms that can be tuned (at the plot scale) than the fine-scale models, leading to variation in the simulation of E across the models (Table 2). The Sperry model performed best and also captured predawn □ observations with high accuracy (Fig. S2). The difference between Sperry and TREES simulations, which include the same fundamental hydraulic structure, is a result of recalibration of the Sperry model to □ measurements after rainfall events or new growing seasons, which TREES did not do. In addition to E, MuSICA predictions of predawn and midday leaf □ averaged (r) 0.88 in piñon and 0.95 in juniper. The error was attributed to insufficient knowledge of below-ground water uptake dynamics, and the assumption of complete refilling whenever xylem pressure became less negative. ED(X) predictions of daily total E improved after calibration of the slope of photosynthesis to stomatal conductance within the Ball–Berry model to fit pretreatment E observations. The resulting model also captured soil □ reasonably well ($r = 0.91$, $P < 0.01$; Fig. S3). The CLM (ED) model was relatively successful at predicting the rapid response of canopy water use to variation in rainfall, but regression fits were not strong, in part because this was the only model to run both species together rather than separately. CLM (ED) simulation of E was limited by a soil □ stress factor that is superimposed on the Ball–Berry estimates of stomatal conductance. The stress factor is nonlinear with respect to water content, which drove the rapid increases and decreases in water use with small changes in soil water.

III. Simulations of hydraulic failure and carbon starvation

1. Hydraulic failure

We compared PLC simulations for both species and treatments to investigate model predictions of hydraulic failure before mortality. The models simulated significantly greater PLC in trees of both species that died during the simulation periods (located on the drought plot) than in those that survived (located on the ambient plot; Fig. 2, $P < 0.001$ for drought vs control, for both species, for all models; using semiparametric regression based on Wand *et al.*, 2009). This is consistent with empirical observations of water uptake and stem native conductivity differences across treatments and species at this site (Plaut *et al.*, 2013; P. Hudson *et al.*, unpublished). Only ED(X) predicted that trees ever experienced 100% PLC. ED(X) assumed that root □ is equal to soil □, but this is false because soil □ dropped to *c.* □8.0 Mpa, while piñon pine xylem □ does not fall much below □3.0 MPa at this site (Plaut *et al.*, 2012; Limousin *et al.*, 2013) or anywhere else in piñon pine's range (West *et al.*, 2007; Breshears *et al.*, 2009). ED(X) simulated reasonable PLC for juniper because the assumption that soil and root □ are equal is nearly met at this site (Plaut *et al.*, 2012). We suspect that the ED(X) PLC estimates for pine may accurately represent below-ground xylem PLC because the soil □ simulations were accurate (Fig. S3) and thus crossover of the Sperry (e.g.) and ED(X) PLC simulations in Fig. 2 may represent the timing of complete loss of K from the soil to the roots.

Amongst the remaining models that simulated PLC, we found that hydraulic processes well beyond the simple tissue-level vulnerability relationships (Eqn 1, Notes S1) were critical to driving PLC. The largest drivers of intermodel variability were the setting of maximum K (because PLC is the loss of conductance relative to the maximum) and simulating root □. The Sperry model was the most highly calibrated one, in part because this was the second iteration of modeling at this site (after Plaut *et al.*, 2012) and it was focused only on hydraulics. It used the maximum simulated hydraulic conductance averaged for surviving trees over the simulation period to set species-specific reference conductance. Predawn leaf □ was simulated to set the minimum root □ (Fig. S2) to avoid assuming the root and soil □ distribution. TREES used a similar approach to estimating root □, but, by contrast, it simply set maximum conductance to the single measured value (tree-specific) before drought treatment initiation in 2007. By using this single value, TREES most likely underestimated maximum conductance and hence simulated unrealistically low PLC (Fig. 2). ED(X) also used a single measured value (species-specific) of hydraulic conductance before drought treatment initiation in 2007 to set maximum conductance. In MuSICA, maximum conductance was calibrated through optimizing the distribution and hydraulic conductivity of fine roots relative to soil properties, to match the predawn □ data before drought. Root □ was then computed dynamically via hydraulic capacitance optimized to match the time lag between tree transpiration and root water uptake estimated from sap flow data.

Table 2 Summary of model performance in comparison of simulated and observed E (per unit sapwood area)

Model	r, P Piñon pine	Juniper
Sperry	0.95, < 0.01	0.99, < 0.01
TREES	0.78, < 0.01	0.71, < 0.01
MuSICA	0.78, < 0.01	0.82, < 0.01
ED(X)	0.61, < 0.01	0.55, < 0.01
CLM(ED)	0.35, $P = 0.87$[a]	

[a]CLM(ED) simulated only pine.

2. Carbon starvation

From treatment initiation until autumn 2011, dying trees had 38 and 44% lower GPP than surviving trees for pine and juniper, respectively ($P < 0.001$ for all models and species). Decreasing GPP with drought is, of course, expected, but it is also a required tenet of

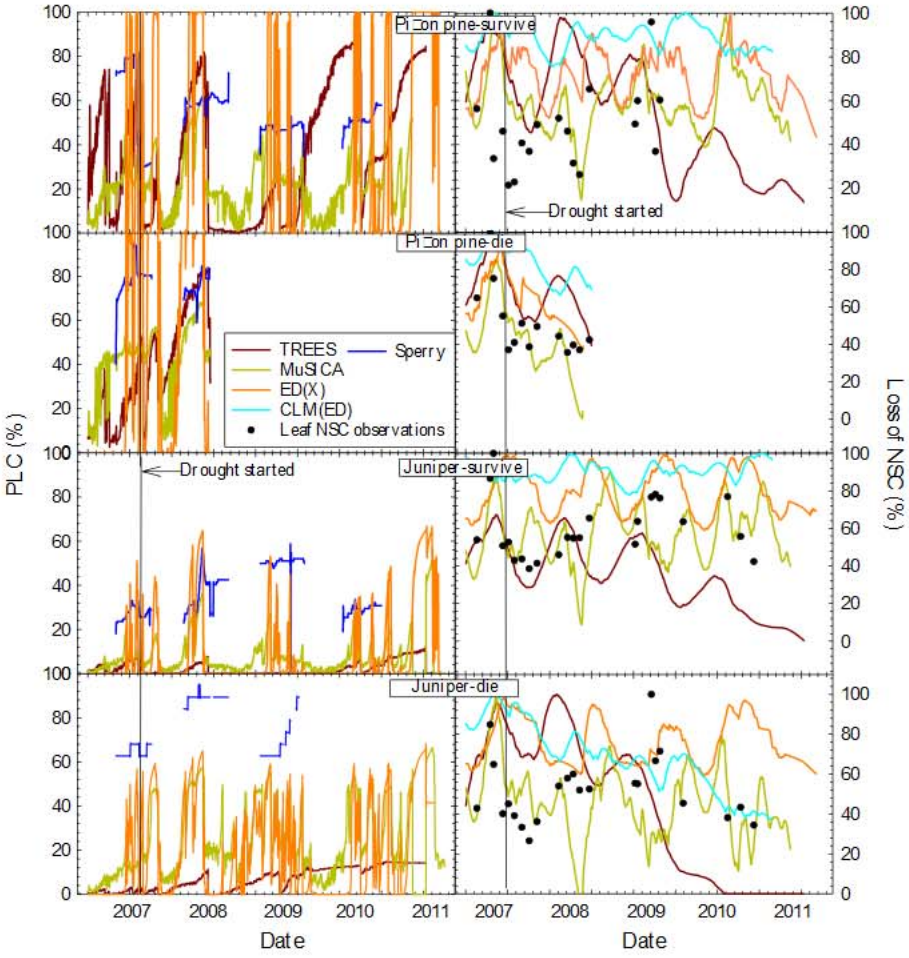

Fig. 2 Simulated percentage loss of conductance (PLC) (left column) and percentage loss of nonstructural carbohydrate (NSC) relative to maximum (right column) by TREES, MuSICA, Sperry (PLC only), ED(X), and CLM(ED) (NSC only). Leaf NSC observations from these plots are also shown. Simulations ended when the mortality threshold was reached (ED(X) and CLM(ED)) or on the date of observation of desiccated canopies (TREES, MuSICA, Sperry; Plaut *et al.*, 2012). Drought treatment was initiated on August 2007 and mean dates of death were August 2008 for piñon pine and June August 2011 for juniper.

carbon starvation (McDowell *et al.*, 2008). The second tenet is that NSC declines. For the same period, all models simulated lower whole-tree NSC stores in trees that died than in those that survived (Fig. 2, $P < 0.001$ for both species). None of the models consistently captured the variation observed in leaf NSC measurements (Fig. 2; the highest r-value was 0.40 for all models); however, we note that comparing observations of leaf NSC to simulations of whole-tree NSC is not a fair test. The large variability amongst models appears to be the result of the wide range of approaches to simulating the dynamics of fluxes into and out of the NSC pool. TREES constrained NSC depletion through simulating maintenance respiration as a direct function of K, but large changes in K still lead to similarly large declines in NSC. MuSICA also simulated low NSC values despite a conservative, source-driven respiration algorithm, with the lowest predicted NSC values found in August 2008 when maximum pine mortality was recorded. Notably, MuSICA allows NSC to decline to zero rather than imposing a minimum threshold. In contrast to smaller-scale models, ED(X) and, to a lesser degree, CLM(ED) predicted relatively small NSC fluctuations because allocation to storage was adjusted to maintain a target residual store of NSC relative to leaf biomass (similar to Fisher *et al.*, 2010). To buffer depletion of NSC storage pools, these models simulate the replacement of tissues, such as foliage and roots, as approaching zero when photosynthesis becomes zero, and ED(X) also down-regulates respiration by 50% when carbon storage crosses a threshold. A noteworthy point is that the general model approach of constraining NSC consumption by reducing allocation to other processes (e.g. Fig. 1) inherently invokes a shift in NSC allocation priorities during drought, which remains a topic of actively growing research (Sala *et al.*, 2012; Stitt & Zeeman, 2012; Wiley & Helliker, 2012).

IV. On thresholds vs duration of stress as drivers of mortality

A common question in the mortality field is: what are the thresholds beyond which mortality is unavoidable? A logical and still standing hypothesis is that 100% PLC and 0% NSC are thresholds for mortality, but there is no evidence to support the notion that these extreme depletions in hydraulic and carbohydrate metabolism are necessary to cause mortality (McDowell *et al.*, 2011; Gruber *et al.*, 2012). By contrast, 1 yr of near-zero stomatal conductance seems to be a shared temporal duration beyond which mortality becomes likely in mature conifer species (Breshears *et al.*, 2009; Plaut *et al.*, 2012; Lévesque *et al.*, 2013).

Because the individual models all demonstrated consistent treatment and species results, we generated multimodel ensembles to investigate the consensus behavior of modeled durations and

absolute thresholds associated with mortality, across a range of model assumptions and approaches (e.g. Sitch *et al.*, 2008; Powell *et al.*, 2013). No clear thresholds were detected when comparing the ensemble simulations to the dates of mortality in August 2008 (pine) and the end of 2011 (juniper, Fig. 3). Simulated piñon pine trees that died in August 2008, 1 yr after installation of the drought treatment, achieved a maximum PLC of *c.* 80% and a minimum NSC of 40% of their starting NSC pool just before mortality. These may be taken as hypothetical thresholds; however, surviving pine trees were simulated to have equally large (or larger) changes in 2011 (Fig. 3) during a regional drought, but did not die (see Section VI for further interpretation of this result). Therefore, there is no evidence from these simulations of a threshold PLC or NSC loss (e.g. 80% and 40% from this example) beyond which mortality is inevitable.

Juniper may be even less likely to have simple mortality thresholds. Juniper trees dropped foliage progressively during drought and exhibited gradual canopy loss from 2007 to 2013 and whole-tree mortality (defined as whole-canopy loss; Gaylord *et al.*, 2013) during 2010–2013 (Plaut *et al.*, 2013). The faster and larger drought responses simulated for piñon pine than for juniper (Fig. 3) were the result of model representations of isohydry and anisohydry for piñon pine and juniper, respectively (West *et al.*, 2007; McDowell *et al.*, 2008; Breshears *et al.*, 2009). These ensemble simulation results are partially consistent with the original predictions of McDowell *et al.* (2008): rather than mechanisms being partitioned between species, the processes of hydraulic failure and carbon starvation appear to co-occur in both species as they were exposed to prolonged, ecosystem-scale precipitation reductions that lead to death. The relatively more isohydric piñon pine progressed down the path of hydraulic failure and carbon starvation ahead of the relatively anisohydric juniper. This result is consistent with iso-anisohydry death trajectories demonstrated empirically in glasshouse-grown seedlings (Mitchell *et al.*, 2013).

All models simulated that trees of both species that died spent significantly more time with relatively high PLC values (Fig. 4, $P < 0.001$ for all models and species, Kolmogorov–Smirnov test; Marsaglia *et al.*, 2003). While the relative values for mean PLC varied substantially between models, these treatment and species results were consistent across all models (Fig. 4), with means for all models of 41 and 63% PLC for surviving and dying pine trees, respectively, and 21 and 32% PLC for surviving and dying juniper trees, respectively, from the date the drought treatment was initiated until death. This consistent result arose primarily from the large treatment differences in soil water availability and species differences in cavitation vulnerability.

Similar to PLC, each model's simulations of NSC suggested trees that died spent greater amounts of time with lower NSC than trees that survived (Fig. 4, $P < 0.001$ for all models and species). Using MuSICA as an example, piñon pine trees that eventually died in the drought plot had only 39% of their maximum NSC reserves, whereas pines that survived on the ambient plot averaged 54% over the same period. These treatment and species differences were also consistent across the models, with means for all models of 76 and 51% of maximum NSC for surviving and dying pine trees, respectively, and mean simulated NSC of 52 and 45% of the maximum for surviving and dying junipers, respectively, from the date of drought treatment onset to the time of death. This consistent result arose primarily because all models simulated a decline in both growth and respiration with drought and ensuing mortality, but this was insufficient to compensate for the even larger photosynthetic reduction (dying pines and junipers had 62 and 57% of the GPP of surviving trees, respectively; $P < 0.01$ for both species), resulting in consistently declining NSC for all trees that ultimately died.

Closer examination of the ensemble model results suggests these models may more realistically simulate NSC trends for the isohydric than for the anisohydric species. In Fig. 5, we have corrected for temporal variation in NSC by plotting the difference between the NSC of dying trees and that of surviving trees, allowing visualization of the relative impact of drought and ensuing mortality on NSC in comparison to trees that survive. A significant trend of decreasing leaf NSC was observed in piñon pine trees

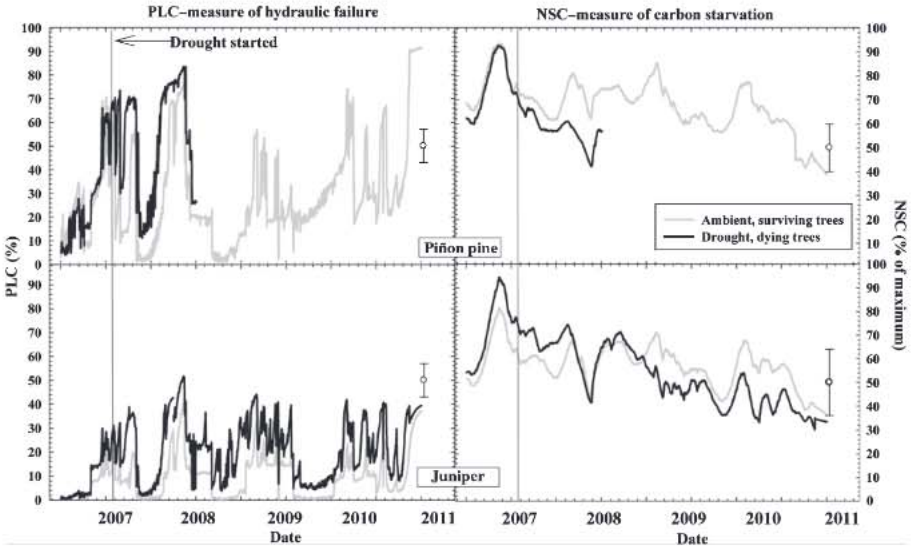

Fig. 3 Model ensemble simulations of percentage loss of conductance (PLC) and percentage nonstructural carbohydrate (NSC) loss for piñon pine and juniper trees in the ambient (surviving) and drought (dying) treatments. The models used are TREES, MuSICA, Sperry, ED(X), and CLM-ED. Ensemble means across all models were created by averaging the daily output for each model, which was the mean of individual tree simulations for Sperry, TREES, and MuSICA, and the daily simulations of the two stands for the dynamic global vegetation models (DGVMs). The mean standard error is shown on the right-hand side of each panel for clarity.

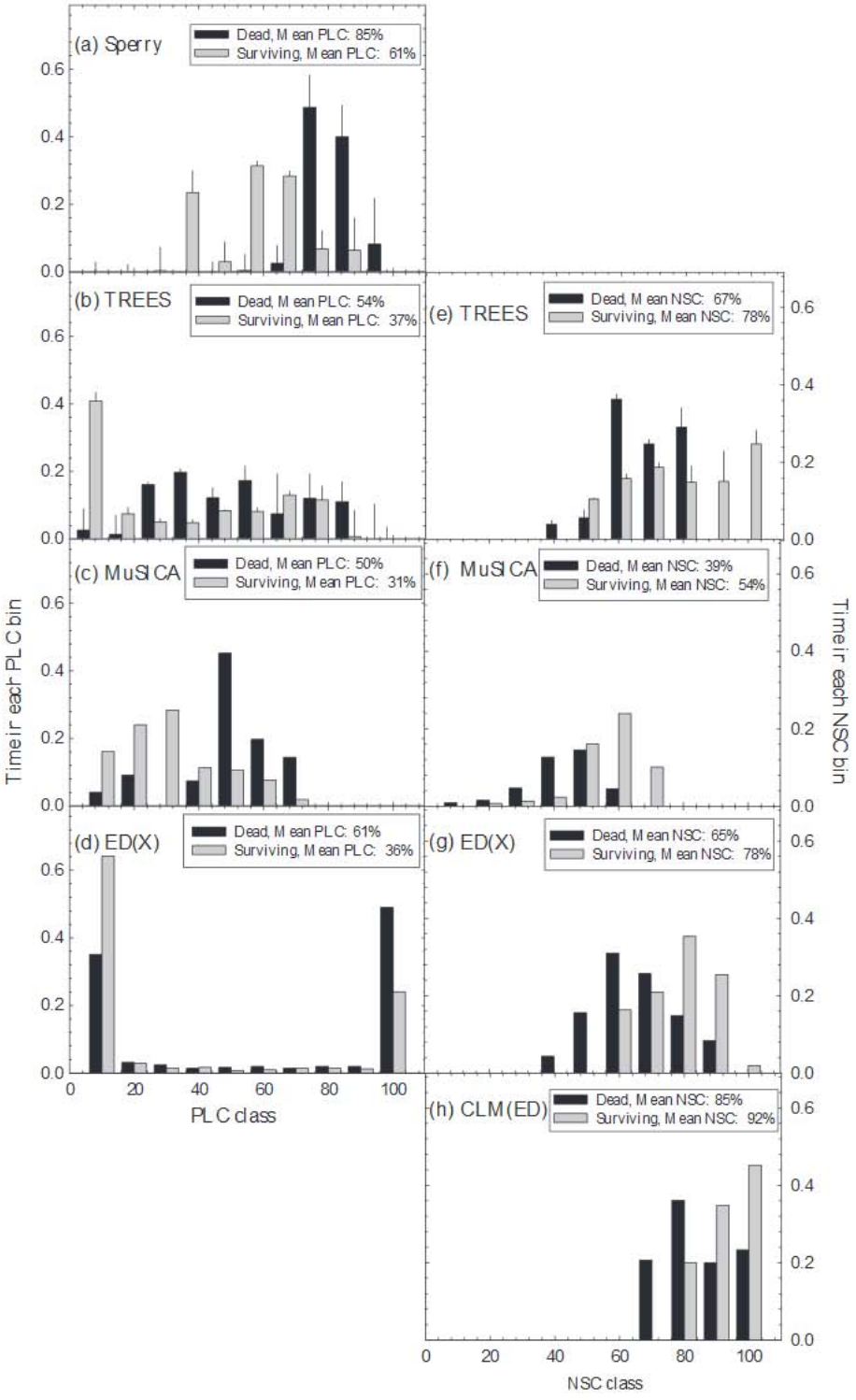

Fig. 4 The frequency of days at percentage loss of conductance (PLC) classes (a–d) and nonstructural carbohydrate (NSC) classes (e–h) over the modeled time period. Black, trees died; gray, trees survived. Panels are offset so each model can be compared. Note that error bars are provided only for models that simulated individual trees.

($r = 0.70$), and this trend was moderately captured by the model ensembles ($r = 0.47$). The models also suggested a decline in NSC for dying junipers, but the observations exhibited a relatively stable NSC storage pool. This may be because of a mismatch of leaf and branch observations (19 and 31% of tree NSC, respectively; Notes S2a) vs whole-tree simulations, and a more rapid leaf shedding in the junipers than was simulated (Gaylord *et al.*, 2013). Thus, a survival strategy of juniper appears to be hydraulic adjustment to reduce leaf area and maintain hydraulic function and NSC pools above critical values (Limousin *et al.*, 2013). It is possible that shifts in relative NSC allocation and depletion between above- and below-ground biomass could have led to this apparent discrepancy between modeled and observed juniper NSC (Hartmann *et al.*, 2013).

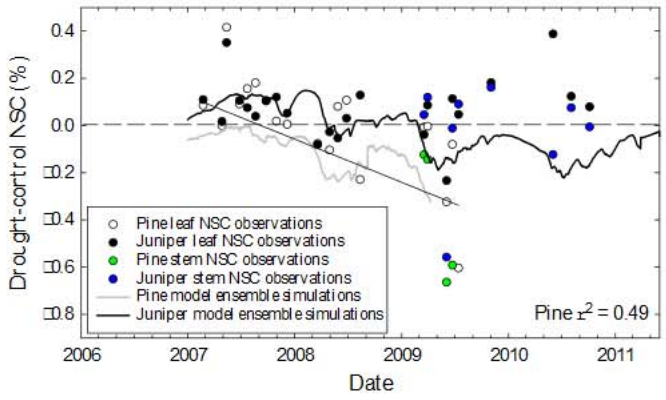

Fig. 5 Ensemble mean nonstructural carbohydrate (NSC) simulations and leaf and branch NSC observations calculated as drought minus control values for each date. Both leaf and branch NSC observations are displayed in the same manner for comparison. Branch observations did not start until 2009. The regression for piñon pine leaf observations is: drought-control NSC (%) = −0.0005 × day + 0.123.

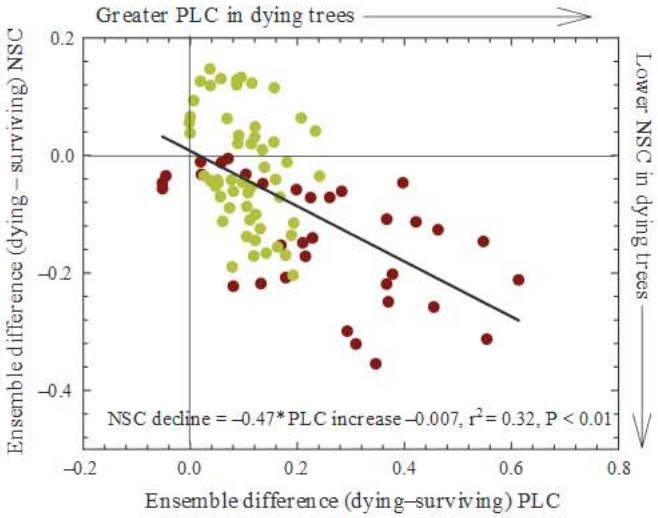

Fig. 6 Model ensemble results of the relationship between the percentage loss of conductance (PLC) difference (%) between dying and surviving trees and the nonstructural carbohydrate (NSC) difference between dying and surviving trees. Negative NSC values indicate that the dying trees had lower NSC content than the surviving trees (right-hand axis). Positive PLC values indicate that dying trees had higher PLC than surviving trees (upper axis). The ensemble model results were grouped into 30 d bins. Models used in the ensemble were TREES, MuSICA, ED(X), and CLM(ED). Piñon pine, brown; juniper, green.

The consistent simulation across all models of greater PLC and reduced NSC in trees that died supports the co-occurrence of hydraulic failure and carbon starvation during drought-induced mortality at this site. This is logical, given that increasing PLC reduces gas exchange and prolongs zero photosynthesis and elevate heat stress (McDowell *et al.*, 2008; Limousin *et al.*, 2013). Chronically low gas exchange rates associated with high PLC could also impair embolism refilling capacity (Zwieniecki & Holbrook, 2009), reduce resin production and pressure (Herms & Mattson, 1992; Gaylord *et al.*, 2013), limit xylem water available for transfer into phloem conduits and hence reduce phloem transport (Hölttä *et al.*, 2009) and turgor loss (Brodribb & Holbrook, 2006). It is from these interactive hydraulic and carbon metabolism processes that the interdependency hypothesis of mortality has arisen (McDowell *et al.*, 2011).

V. Interdependence of hydraulic failure and carbon starvation

There are many feedbacks between carbohydrate and hydraulic dynamics that can accelerate or buffer the rate of mortality during drought (Fig. 1; Hummel *et al.*, 2010; McDowell *et al.*, 2011; Mueller *et al.*, 2011). Simulated PLC and NSC should, in theory, capture many of these feedbacks, regardless of the spatial or temporal scale of simulation. Consistent with this, correlation of the ensemble results of PLC and NSC simulations from Fig. 3 revealed that modeled periods of depleted NSC were associated with simulated increases in PLC (Fig. 6). In this analysis, the daily difference between ensemble predictions of the ambient (surviving) and drought (dying) trees is calculated for both NSC and PLC. The mean daily difference for 30 d periods was calculated to allow for temporal displacement between cause-and-effect relationships of PLC and NSC. Both species fall along the same trend. This result is consistent with an interdependency of mechanisms underlying vegetation mortality, starting with strong stomatal impacts on photosynthesis (Martínez-Vilalta *et al.*, 2002; McDowell *et al.*, 2011). Strictly quantifying the interdependence of these factors is a big empirical challenge, but it can be simulated using highly detailed process models such as FINNSIM.

Our goals for the FINNSIM simulations of whole-tree xylem and phloem function were, first, to investigate the hypothesis that phloem transport ceases during drought as a result of failure of the interdependent hydraulic-carbohydrate system (McDowell & Sevanto, 2010; Sala *et al.*, 2010; McDowell, 2011) and, secondly, to apply the model to investigate potential mechanisms underlying the hydraulic results and carbohydrate costs of maintaining xylem function (Zwieniecki & Holbrook, 2009). Using driving parameters most consistent with the observations and results of the other models, FINNSIM simulated the failure of phloem transport (represented here as the phloem turgor gradient from top to bottom of the canopy – the most direct and measurable trait of phloem function) in both species during the seasonal drought in 2008 (Fig. 7). The model simulated juniper to have lower turgor than pine, and trees of both species that died had lower turgor than those that survived. For the relatively anisohydric juniper, photosynthesis continues down to −6 MPa (Limousin *et al.*, 2013), which provides sugars to aid in maintaining phloem pressure (Hölttä *et al.*, 2009; Sevanto *et al.*, 2013), but the lack of water availability to the phloem with xylem Ψ exceeding −8 MPa during drought (Plaut *et al.*, 2012) forced a complete cessation of juniper phloem function for extended periods (Fig. 7). By contrast, phloem transport was not predicted to be constrained by water availability in piñon pine as a result of its relatively isohydric behavior, which maintained xylem Ψ significantly higher (> −3MPa) than values that would impair phloem function. Pine phloem transport is constrained only by NSC availability, which becomes limiting

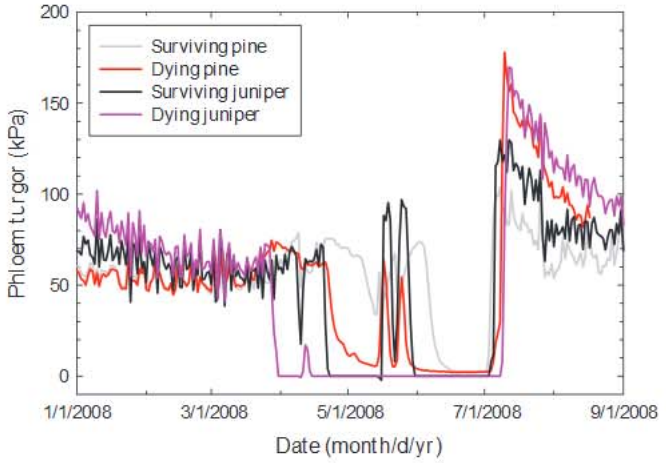

Fig. 7 FINNSIM simulations of the phloem turgor gradient from the upper canopy to the base of the stem. Turgor is the simplest and most testable metric of phloem transport, and simulations of phloem flux rates are nearly identical to turgor gradient simulations. The timescale was reduced to focus on January September 2008 to highlight the dynamics proceeding pine mortality in August 2008. The phloem turgor gradient declines and hence nonstructural carbohydrate (NSC) transport ceases earlier in juniper than in piñon pine, largely as a result of the larger decline in xylem water potential in junipers and hence water available to the phloem. This effect is magnified for droughted junipers that die by 2011. Droughted pines that die in 2008 show a reduced phloem turgor as a result of a lack of NSC-based solutes to drive transport; xylem water potentials are never sufficiently low to impair phloem transport in dying or surviving pines.

during extended periods of zero gas exchange (Limousin *et al.*, 2013). It will require empirical tests to determine if such a decline in phloem function actually matters to survival when GPP is near zero and there is no photosynthate to transport.

We extended the FINNSIM simulations to examine xylem refilling and its potential impacts on hydraulics and carbohydrate balance. We varied the rate of refilling and the amount of sucrose irreversibly consumed in refilling, as the precise refilling mechanism and its associated metabolic costs are not known (Zwieniecki & Holbrook, 2009). The rate of refilling determined the progression of PLC over time (Fig. 8a). In some cases, no refilling rates were sufficient to repair the loss of conductance.

Faster refilling kept PLC lower (Fig. 8a), but increased the carbon costs of refilling, especially when we assumed some fraction of sucrose used in refilling was not recycled (empirical values on how much NSC is lost from refilling do not exist). Despite carbon loss to refilling, embolism repair consumed only a minor portion of the plant's carbon budget. Even under the unlikely scenario of the highest refilling rates and with all sucrose used in refilling lost (0% recycled), the carbon cost of refilling was at most 40% of the annual cost of leaf respiration (Fig. 8b,c), or 10% of the total NSC in the plant (Fig. 8d). These results suggest that the carbon cost of refilling is unlikely to be large relative to the entire plant carbon budget; however, it may be a large amount of carbon for plants undergoing the late stages of carbon starvation (McDowell, 2011). This extra cost could, in theory, be responsible for the overestimates of NSC by most models (Fig. 2), as these models all assumed no carbon costs for refilling or maintaining phloem function.

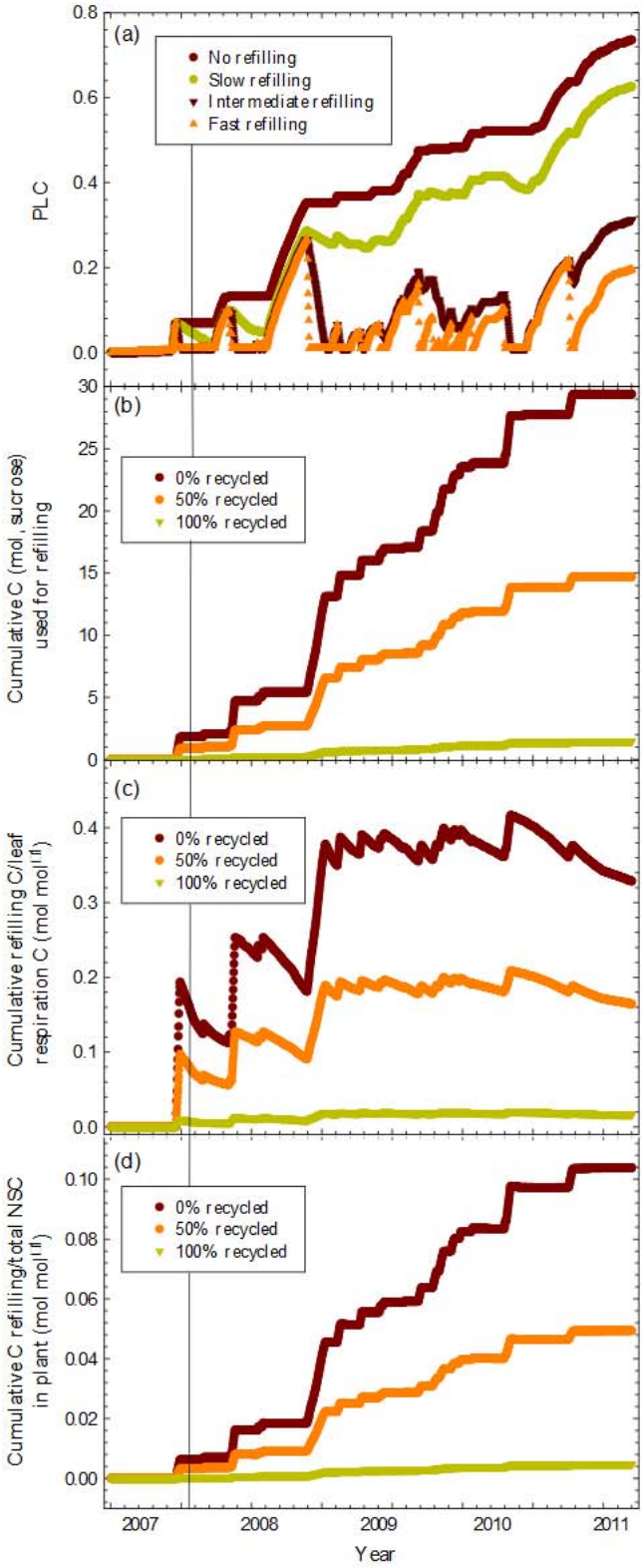

Fig. 8 Xylem refilling modeled by FINNSIM. (a) Proportion loss of conductance (PLC) as a function of refilling rate. (b) Cumulative carbon per plant (mol) used for refilling as a function of the recycling rate of sucrose. (c) Ratio of the cumulative refilling carbon costs relative to cumulative leaf respiration (Notes S2b, S3). (d) The ratio of cumulative carbon costs of refilling relative to the total amount of nonstructural carbohydrate (NSC) within the plants.

VI. Next-generation, traditional, and empirical models

The treatment and species differences across models for PLC and NSC (Figs 3–8) are consistent with mortality occurring through the interdependence of hydraulic failure and carbon starvation at the stomatal, xylem/phloem, and below-ground interfaces (McDowell *et al.*, 2011). It is clear that simulating hydraulic failure and carbon starvation is insufficient to accurately predict mortality, however, because of the significant impact of attacking biotic agents during drought on mortality (Raffa *et al.*, 2008). This is exemplified by the ED(X) simulations (Fig. 9a). ED(X) correctly simulated the piñon pine mortality that occurred in 2008 (simulations were within the 95% confidence interval of the observation) in the presence of a bark beetle outbreak (*Ips* species; Plaut *et al.*, 2012; Gaylord *et al.*, 2013) with an assumed NSC threshold, but incorrectly simulated mortality of the (still living) pine trees on the ambient plot during the record-setting, severe regional drought in 2011 (Mu *et al.*, 2013) during which there was no local outbreak of beetles (Fig. 9a; Limousin *et al.*, 2013). There

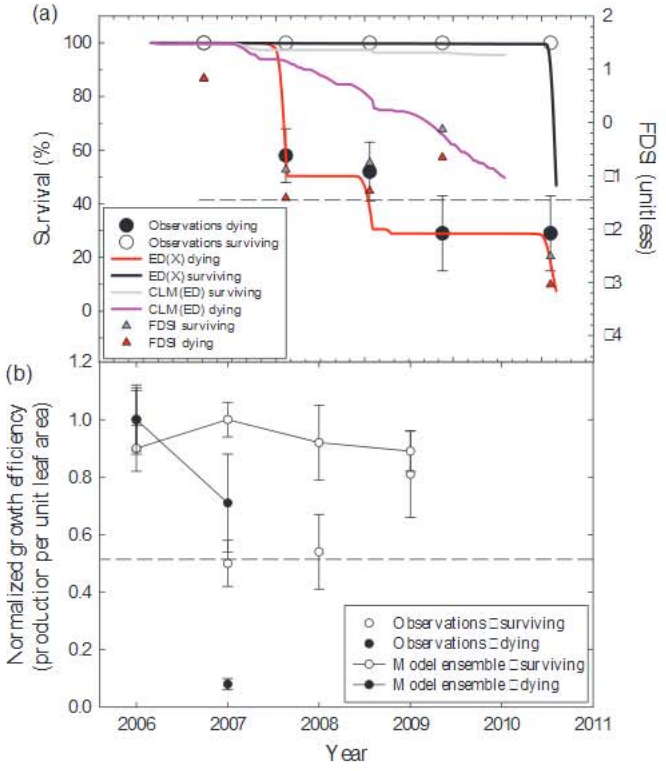

Fig. 9 (a) Observations of piñon pine mortality and survival and simulations by the dynamic global vegetation models (DGVMs) ED(X) and CLM(ED), and predictions using the empirically based Forest Drought Severity Index (FDSI, Williams *et al.*, 2013), assuming the FDSI value associated with mortality during the 1590s megadrought (1.41) is equal to 100% mortality (dashed line). (b) Observations and model ensemble (TREES, MuSICA, ED (X), and CLM(ED)) simulations of growth efficiency. The dashed line represents the uppermost possible mortality prediction threshold using nearly all thresholds found in traditional DGVMs (McDowell *et al.*, 2011), including thresholds based on constant background rates, climate envelopes, size or age thresholds, growth efficiency, net primary production, shading, and heat stress. Bars represent SE.

are currently no published DGVMs or process models that include biotic attack in mortality simulations (e.g. Fig. 1, McDowell *et al.*, 2011). There are, however, models of pathogen population dynamics that utilize climate data and estimates of forest stress (e.g. Biesinger *et al.*, 2000) that could potentially be coupled to the NSC or new defense modules in DGVMs (e.g. Fig. 1). This approach may be useful at our site. An anomalous January cold event (29.0 on site) that exceeded the cold temperature survival threshold of *Ips* (21 ; Chansler, 1966) occurred in 2011, whereas the coldest temperatures in 2007 and 2008 on site did not fall below 15.2 . Thus, despite greater physiological carbon starvation and hydraulic failure than for trees that died in 2008, remaining pine trees survived the drought in 2011, indicating that the mortality thresholds (e.g. absolute values or duration of NSC or PLC values) may vary with the presence of attacking agents (Raffa *et al.*, 2008). Furthermore, there is strong evidence from these same experimental plots that average NSC is a reasonable predictor of mortality ($r^2 = 0.77$; L. T. Dickman, unpublished) and thus a logical link exists both within the model framework and from empirical data. For near-term predictions, such models can be linked to remotely sensed estimates of mortality, to serve as initiation for further insect outbreaks (Wulder *et al.*, 2006).

At the far end of the spectrum of model complexity, approaches using empirical relationships between mortality and indices such as meteorological drought are appealing (e.g. Wulder *et al.*, 2006; Williams *et al.*, 2013). These approaches risk oversimplification and resulting loss of accuracy when run into the future; however, given the large amount of data that can go into empirical models, they may be highly accurate in the near term (100 yr). To test if a simple, empirical approach could capture mortality in our study, we used a new empirical relationship between cold-season precipitation, summer evaporative demand, and tree-ring-based growth and mortality estimates (the Forest Drought Severity Index, FDSI) to predict mortality (Fig. 9a; Williams *et al.*, 2013). An FDSI value of 1.41 was associated with widespread forest mortality in the 1590s in the southwestern USA (Betancourt *et al.*, 1993; Brown & Wu, 2005), including for piñon pine trees, and thus we use 1.41 as a hypothesized value beyond which mortality may occur. Similar to ED(X), the FDSI approach correctly predicted piñon pine mortality in 2008, but incorrectly predicted mortality in 2011. FDSI is an annual metric, which is consistent with the observation that mature, field-grown conifers can survive *c.* 12 months without positive photosynthesis (Breshears *et al.*, 2009; McDowell, 2011; Lévesque *et al.*, 2013). Thus, both the highly mechanistic and highly empirical approaches suffer from similar errors of not accounting for all processes, in this case, bark beetle attack dynamics.

An intermediate approach is to apply the numerous traditional DGVM mortality indices (McDowell *et al.*, 2011). These simpler algorithms are appealing because they are already in place in the DGVMs and can be measured relatively easily. In our rather unnatural experimental manipulation (precipitation reduction without concomitant temperature rise as typically occurs in drought; e.g. Breshears *et al.*, 2005), the traditional mechanisms

of constant background mortality, climate envelopes, heat stress, size and age thresholds, and shading were all ineffective to predict mortality because the trees did not cross any temperature, size, or shading thresholds during this study. Simulations of NPP and growth efficiency (production per unit leaf area; Waring & Pitman 1985, Notes S4) did capture the species and treatment trends correctly, but like the other indices, they overestimated survival because the assumed mortality thresholds were not exceeded in the simulations (Fig. 9b). Model predictions across the range of complexity spectrums can be integrated with models of biotic agents (both mechanistic and empirical), and all model types should then be evaluated at regional scales (e.g. Wulder *et al.*, 2006) to ensure they can obtain the correct answers for the correct reasons. These conclusions are based on one study site with two sympatric species, but may be representative of a global science challenge owing to our limited knowledge of fundamental mortality mechanisms and the importance of biotic attack agents in mortality globally (Raffa *et al.*, 2008; Bentz *et al.*, 2010; McDowell *et al.*, 2011; Hicke *et al.*, 2012).

VII. A path forward

Our analysis has revealed that, regardless of scale, all models suggest that the duration of hydraulic impairment and low NSC stocks is associated with mortality; that the stomatal, phloem, and below-ground carbon and water interdependences were all important during simulated drought and mortality; and that mechanistic, traditional, and empirical modeling approaches all have similar vulnerability to processes not yet considered, such as biotic agent populations. These results emerged despite the various ways that models simulated and parameterized the hydraulic and carbohydrate systems, partly because of a fairly common, emergent simulation framework (Fig. 1). This study used an international set of models, but only a single experiment with two species within the traditional Needleleaf Evergreen Tree PFT (e.g. Jiang *et al.*, 2013), and thus an obvious next step is a similar test in another PFT, perhaps one with contrasting hydraulics to needleleaf evergreens (e.g. deciduous broadleaf trees; Mitchell *et al.*, 2013).

Developing predictive tools of forest mortality is faced with the challenge of balancing the traditional approach of adding complexity to existing models with the need to minimize complexity and uncertainty and maximize the ability to test and constrain the models. Existing models have much of the necessary processes considered critical to plant mortality, based on theory (McDowell *et al.*, 2008, 2011) and relatively consistent empirical evidence from glasshouse and field mortality studies on angiosperms and gymnosperms (Anderegg *et al.*, 2012; Plaut *et al.*, 2012, 2013; Galvez *et al.*, 2013; Limousin *et al.*, 2013; Mitchell *et al.*, 2013; Quirk *et al.*, 2013; Sevanto *et al.*, 2013). In particular, the creation and subsequent modification of models that integrate energy balance, physiology, and the demographics and structure of vegetation (Moorcroft *et al.*, 2001; Fisher *et al.*, 2010; Powell *et al.*, 2013) have allowed integration of many of the hypothesized mortality processes that scale from the cell to the region (McDowell *et al.*, 2011). Thus, there is a strong rationale to continue using these models for investigation of processes.

Previous multimodel drought experiment evaluations in the Amazon revealed that simulation of both carbon and water dynamics, and subsequent mortality, was relatively accurate for the control plots but generally failed in the drought plots (Galbraith *et al.*, 2010; Powell *et al.*, 2013). Our study also revealed the challenges of simulating these processes, down to the tissue scale, and also revealed additional uncertainties pertinent to our current simulation framework (e.g. Fig. 1) within this pine–juniper woodland. All of the tested models, regardless of scale, require accurate parameterization of root □ in order to correctly estimate *K*, PLC, and all downstream hydraulic and carbohydrate properties (e.g. Fig. 1). This can be achieved through knowledge of rooting depth, minimum xylem □, and soil–root hydraulic conductance. Alternatively, highly tuned simulations of root □, such as we did in the Sperry model (Fig. S2), may allow simplification for regional-scale parameterization. Root □ was among the largest uncertainties identified by our group because it caused rapid and large impacts on *K*, PLC, stomatal conductance, GPP, and NSC storage. While this remains to be thoroughly tested, global models should be able to utilize PFT-specific estimates of rooting depth (e.g. Schenk & Jackson, 2005) and maps of soil depth and texture classification, along with PFT-specific vulnerability curves and □ estimates for roots, trunks, branches, and leaves (Kattge *et al.*, 2011; Choat *et al.*, 2012) and minimum leaf□ to improve simulations. On the carbon side, all models require improved understanding of carbohydrate storage regulation (e.g. Sala *et al.*, 2012). NSC content is the net product of GPP and multiple sinks, including storage, respiration, growth, and defense, and linking each of these allocations through empirical and model-based research is critical to many fields of research (Stitt & Zeeman, 2012; Richardson *et al.*, 2013). Our model–experiment comparison revealed these processes as essential to mortality, and improving our knowledge of these mechanisms should allow a more rigorous interpretation of the underlying physiological mechanisms of carbon–water coupling during drought (Mueller *et al.*, 2011).

For models intended for simulation in field settings, representation of biotic attack and defense against biotic attack is critical (e.g. Fig. 9a). Statistical and mechanistic population dynamics models of biotic agents (e.g. Hicke *et al.*, 2007; Magori *et al.*, 2009) should be considered for integration into DGVMs. Integrated landscape-scale models of vegetation susceptibility and insect population dynamics will allow the links among climate, forest vulnerability, and outbreaks to be investigated, and can subsequently be used to parameterize DGVMs. Models of biotic attack and forest vulnerability will require evaluation datasets that incorporate patterns of large-scale mortality, climate, species, soil conditions, and, most critically, attack rates of biotic agents, in order to capture the real-world heterogeneity in edaphic, species, and disturbance drivers (Luo *et al.*, 2012). Spatially distributed datasts are simultaneously critical for DGVMs, for which the smallest scale of simulation is the stand and hence replicated tests require evaluation at larger spatial scales. Such mortality benchmarks do not yet exist outside of inventory data, but potential exists for using remotely sensed approaches (Wulder *et al.*, 2006; Huang *et al.*, 2010; Garrity *et al.*, 2012; Kennedy *et al.*, 2012; Meddens *et al.*, 2012; Mu *et al.*, 2013). These evaluation tests serve the

additional benefits of providing fundamental knowledge of climate–mortality relationships, from which near-term (*c.* 50 yr) mortality forecasts can be generated (e.g. Fig. 9a and Williams *et al.*, 2013).

VIII. Conclusions

Next-generation models of vegetation physiology are advancing rapidly at scales ranging from individual plants to a global level. Here, all models predicted depletions in NSC pools and increases in PLC in both piñon pine and juniper trees that died within 1–5 yr of a sustained *c.* 45% reduction in precipitation. Model results suggested that mortality depended on the time trees spent with extensive hydraulic failure or carbon starvation, rather than on specific thresholds *per se*. Interdependency of carbon and water was supported by each model. The consistency of these results is encouraging, but substantial research is required before model predictions are reliable in the absence of significant empirical constraints, that is, in future scenarios. Next-generation process models, traditional process model metrics of mortality, and empirical estimates of mortality all suffer from assumptions that were not met in this study, for example the presence of bark beetles. Models representing a wide range of alternative hypotheses must be applied and rigorously evaluated to progress our understanding of the processes underlying tree mortality. Representation of below-ground hydraulic function, NSC dynamics, vegetation defense, and population dynamics of biotic attack agents emerged as critical mechanisms requiring better understanding and modeling. Reducing uncertainty in mortality modeling is critical to better forecasting of future terrestrial impacts as our climate continues to change.

Acknowledgements

We thank the New Phytologist Trust and Trustees for funding in support of the workshop 'A multi-scale model investigation of the mechanisms of drought-induced vegetation mortality' held in Santa Fe, New Mexico, in November 2011. Additional support was provided by the Department of Energy-Office of Science, and LANL-LDRD.

References

Adams HD, Guardiola-Claramonte M, Barron-Gafford GA, Villegas JC, Breshears DD, Zou CB, Troch PA, Huxman TE. 2009. Temperature sensitivity to drought-induced tree mortality portends increased regional die-off under global-change-type drought. *Proceedings of the National Academy of Sciences, USA* **106**: 7063 7066.

Allen CD, Macalady AK, Chenchouni H, Bachelet D, McDowell N, Vennetier M, Kitzberger T, Rigling A, Breshears DD, Hogg EH et al. 2010. A global overview of drought and heat-induced tree mortality reveals emerging climate change risks for forests. *Forest Ecology and Management* **259**: 660 684.

Allison I, Bindoff NL, Bindschadler RA, Cox PM, de Noblet N, England MH, Francis JE, Cruber N, Haywood AM, Karoly DJ et al. 2009. *The Copenhagen diagnosis 2009: updating the world on the latest climate science.* Oxford, UK: The University of New South Wales Climate Change Research Centre.

Amthor J, McCree KJ. 1990. Carbon balance of stressed plants: a conceptual model for integrating research results. *Plant Biology* **12**: 1 15.

Anderegg WRL, Berry JA, Smith DD, Sperry JS, Anderegg LDL, Field CB. 2012. The roles of hydraulic and carbon stress in a widespread climate-induced forest die-off. *Proceedings of the National Academy of Sciences, USA* **109**: 233 237.

Arora VK, Boer GJ, Friedlingstein P, Eby M, Jones CD, Christian JR, Bonan G, Bopp L, Brovkin V, Cadule P et al. 2013. Carbon-concentration and carbon-climate feedbacks in CMIP5 Earth system models. *Journal of Climate*. doi:10.1175/JCLI-D-12-00494.1.

Beck PSA, Juday GP, Alix C, Barber VA, Winslow SE, Sousa EE, Heiser P, Herriges JD, Goetz SJ. 2011. Changes in forest productivity across Alaska consistent with biome shift. *Ecology Letters* **14**: 373 379.

Bentz BJ, Régnière J, Fettig CJ, Hansen EM, Hayes JL, Hicke JA, Kelsey RG, Negrón JF, Seybold SJ. 2010. Global climate change and bark beetles of the Western United States and Canada: direct and indirect effects. *BioScience* **60**: 602 613.

Betancourt JL, Pierson EA, Rylander KA, Fairchild-Parks JA, Dean JS. 1993. Influence of history and climate on New Mexico piñon-juniper woodlands. In: Aldon AF, Shaw DW, eds. *Managing Pinon juniper ecosystems for sustainability and social needs.* USDA Forest Service General Technical Report RM-236. Fort Collins, CO, USA: Rocky Mountain Forest and Range Experiment Station, 42 62.

Biesinger Z, Powell J, Bentz B, Logan J. 2000. Direct and indirect parameterization of a localized model for the mountain pine beetle lodgepole pine system. *Ecological Modelling* **129**: 273 296.

Bonan GB. 2008. Forests and climate change: forcings, feedbacks, and the climate benefits of forests. *Science* **320**: 1444 1449.

Bonan GB, Oleson KW, Fisher RA, Lasslop G, Reichstein M. 2012. Reconciling leaf physiological traits and canopy flux data: use of the TRY and FLUXNET databases in the Community Land Model version 4. *Journal of Geophysical Research* **117**: G02026.

Breshears DD, Cobb NS, Rich PM, Price KP, Allen CD, Balice RG, Romme WH, Kastens JH, Floyd ML, Belnap J et al. 2005. Regional vegetation die-off in response to global-change-type drought. *Proceedings of the National Academy of Sciences, USA* **102**: 15144 15148.

Breshears DD, Myers OB, Meyer CW, Barnes FJ, Zou CB, Allen CD, McDowell NG, Pockman WT. 2009. Tree die-off in response to global-change-type drought: mortality insights from a decade of plant water potential measurements. *Frontiers in Ecology and the Environment* **7**: 185 189.

Brodribb TJ, Holbrook NM. 2006. Declining hydraulic efficiency as transpiring leaves desiccate: two types of response. *Plant, Cell & Environment* **29**: 2205 2215.

Brown PM, Wu R. 2005. Climate and disturbance forcing of episodic tree recruitment in a southwestern ponderosa pine landscape. *Ecology* **86**: 3030 3038.

Carnicer J, Coll M, Ninyerola M, Pons X, Sánchez G, Peñuelas J. 2011. Widespread crown condition decline, food web disruption, and amplified tree mortality with increased climate change-type drought. *Proceedings of the National Academy of Sciences, USA* **108**: 1474 1478.

Chansler JF. 1966. Cold hardiness of two species of *Ips* beetles. *Journal of Forestry* **64**: 622624.

Chapin FS, Schulze ED, Mooney HA. 1990. The ecology and economics of storage in plants. *Annual Review of Ecology and Systematics* **21**: 423 447.

Choat B, Jansen S, Brodribb TJ, Cochard H, Delzon S, Bhaskar R, Bucci SJ, Field TS, Gleason SM, Hacke UG et al. 2012. Global convergence in the vulnerability of forests to drought. *Nature* **491**: 752 755.

Cowan IR, Troughton JH. 1971. The relative role of stomata in transpiration and assimilation. *Planta* **97**: 325 336.

Cox PM, Huntingford C, Harding RJ. 1998. A canopy conductance and photosynthesis model for use in a GCM land surface scheme. *Journal of Hydrology* **212**: 79 94.

Davis SD, Ewers FW, Sperry JS, Portwood KA, Crocker MC, Adams GC. 2002. Shoot dieback during prolonged drought in *Ceanothus* (Rhamnaceae) chaparral of California: a possible case of hydraulic failure. *American Journal of Botany* **89**: 820 828.

Dietze MC, Moorcroft PR. 2012. Tree mortality in the eastern and central United States: patterns and drivers. *Global Change Biology* **17**: 3312 3326.

Domec J-C, Ogée J, Noormets A, Jouangy J, Gavazzi M, Treasure E, Sun G, McNulty S, King JS. 2012. Interactive effects of nocturnal transpiration and

climate change on the root hydraulic redistribution and carbon and water budgets of Southern US pine plantations. *Tree Physiology* **32**: 707 723.

Fisher R, McDowell N, Purves D, Moorcroft P, Sitch S, Cox P, Huntingford C, Meir P, Woodward FI. 2010. Assessing uncertainties in a second-generation dynamic vegetation model caused by ecological scale limitations. *New Phytologist* **187**: 666 681.

Friedlingstein P, Cox P, Betts R, Bopp L, von Bloh W, Brovkin V, Cadule P, Doney S, Eby M, Fung I et al. 2006. Climate-carbon cycle feedback analysis: results from the C^4MIP model intercomparison. *Journal of Climate Change* **19**: 3337 3353.

Galbraith D, Levy PE, Sitch S, Huntingford C, Cox P, Williams M, Meir P. 2010. Multiple mechanisms of Amazonian forest biomass losses in three dynamic global vegetation models under climate change. *New Phytologist* **187**: 647 665.

Galvez DA, Landhäusser SM, Tyree MT. 2013. Low root reserve accumulation during drought may lead to winter mortality in poplar seedlings. *New Phytologist* **198**: 139 148.

Garrity SR, Allen CD, Brumby S, Cai DM, Gangodagamage C, McDowell NG. 2013. Quantifying drought-induced tree mortallity in a piñon-juniper woodland using multitemporal high spatial resoltuion satellite imagery. *Remote Sensing of Environment* **129**: 54 65.

Gaylord ML, Kolb TE, Pockman WT, Plaut JA, Yepez EA, Macalady AK, Pangle RE, McDowell NG. 2013. Drought predisposes piñon juniper woodlands to insect attacks and mortality. *New Phytologist* **198**: 567 578.

Gruber A, Pirkebner D, Florian C, Oberhuber W. 2012. No evidence for depletion of carbohydrate pools in Scots pine (*Pinus sylvestris* L.) under drought stress. *Plant Biology* **14**: 142 148.

Hartmann H, Trumbore S, Ziegler W. 2013. Lethal drought leads to reduction in nonstructural carbohydrates (NSC) in Norway spruce tree roots but not in the canopy. *Functional Ecology* **27**: 413 427.

Herms DA, Mattson WJ. 1992. The dilemma of plants: to grow or defend. *Quarterly Review of Biology* **67**: 283 335.

Hicke JA, Allen CS, Desai AR, Dietze MC, Hall RJ, Hogg EH, Kashian DM, Moore D, Raffa KF, Sturrock RN et al. 2012. Effects of biotic disturbances on forest carbon cycling in the United States and Canada. *Global Change Biology* **18**: 7 34.

Hicke JA, Jenkins JC, Ojima DS, Ducey M. 2007. Spatial patterns of forest characteristics in the western United States derived from inventories. *Ecological Applications* **17**: 2387 2402.

Hickler T, Prentice IC, Smith B, Sykes MT, Zaehle S. 2006. Implementing plant hydraulic architecture within the LPJ Dynamic Global Vegetation Model. *Global Ecology and Biogeography* **15**: 567 577.

Hoch G, Richter A, Körner C. 2003. Non-structural carbon compounds in temperate forest trees. *Plant, Cell & Environment* **26**: 1067 1081.

Hölttä T, Cochard H, Nikinmaa E, Mencuccini M. 2009. Capacitive effect of cavitation in xylem conduits: results from a dynamic model. *Plant, Cell & Environment* **32**: 10 21.

Hölttä T, Vesala T, Sevanto S, Perämäki M, Nikinmaa E. 2006. Modeling xylem and phloem water flows in trees according to cohesion theory and Münch hypothesis. *Trees* **20**: 67 78.

Huang C-Y, Asner GP, Barger NN, Neff JC, Floyd ML. 2010. Regional aboveground live carbon losses due to drought-induced tree dieback in piñon-juniper ecosystems. *Remote Sensing of Environment* **114**: 1471 1479.

Hubbard RM, Ryan MG, Stiller V, Sperry JS. 2001. Stomatal conductance and photosynthesis vary linearly with plant hydraulic conductance in ponderosa pine. *Plant, Cell & Environment* **24**: 113 121.

Hummel I, Pantin F, Sulpice R, Piques M, Rolland G, Dauzat M, Christophe A, Pervent M, Bouteille□M,Stitt M et al. 2010. Arabidopsis plants acclimate to water deficit at low cost through changes of carbon usage: an integrated perspective using growth, metabolite, enzyme, and gene expression analysis. *Plant Physiology* **154**: 357 372.

Hurtt GC, Moorcroft PR, Pacala SW, Levin SA. 1998. Terrestrial models and global change: challenges for the future. *Global Change Biology* **4**: 581 590.

Jiang X, Raucher S, Ringler TD, Lawrence D, Williams AP, Allen C, Steiner A, Cai DM, McDowell NG. 2013. Predicted future changes in vegetation in Western North America in the 21st century. *Journal of Climate* **26**: 3671 3687.

Kattge J, Díaz S, Lavorel S, Prentice IC, Leadley P, Bönisch G, Garnier E, Westoby M, Reich PB et al. 2011. TRY a global database of plant traits. *Global Change Biology* **17**: 2905 2935.

Kennedy RE, Yang Z, Cohen WB, Pfaff E, Braaten J, Nelson P. 2012. Spatial and temporal patterns of forest disturbance and regrowth witin the area of the Northwest Forest Plan. *Remote Sensing of Environment* **122**: 117 133.

Kurz WA, Stinson G, Rampley GJ, Dymond CC, Neilson ET. 2008. Risk of natural disturbances makes future contribution of Canada's forests to the global carbon cycle highly uncertain. *Proceedings of the National Academy of Sciences, USA* **105**: 1551 1555.

Le Roux X, Lacointe A, Escobar-Guttiérrez A, Les Dizès S. 2001. Carbon-based models of individual tree growth: a critical appraisal. *Annals of Forest Science* **58**: 469 506.

Lévesque M, Saurer M, Siegwolf R, Eilmann B, Brang P, Bugmann H, Rigling A. 2013. Drought response of five conifer species under contrasting water availability suggests high vulnerability of Norway spruce and European larch. *Global Change Biology*. doi:10.1111/gcb.12268.

Lewis SL, Brando PM, Phillips OL, van der Heijden GM, Nepstad D. 2011. The 2010 Amazon drought. *Science* **331**: 554.

Limousin JM, Bickford CP, Dickman LT, Pangle RE, Hudson PJ, Boutz AL, Gehres N, Osuna JL, Pockman WT, McDowell NG. 2013. Regulation and acclimation of leaf gas-exchange in a piñon-juniper woodland exposed to three different precipitation regimes. *Plant, Cell & Environment*. doi:10.1111/pce.12089.

Liu H, Williams AP, Allen CD, Guo D, Wu X, Anenkhonov OA, Liang E, Qi Z, Sandanov DV, Korolyuk AY et al. 2013. Rapid warming accelerates tree growth decline in semi-arid forests in Inner Asia. *Global Change Biology* **19**: 2500 2510.

Loranty MM, Mackay DS, Ewers BE, Traver E, Kruger EL. 2010. Competition for light between individual trees lowers reference canopy stomatal conductance: results from a model. *Journal of Geophysical Research - Biogeosciences* **115**: G04019.

Luo Y, Randerson J, Abramowitz G, Bacour GC, Blyth EM, Carvalhais N, Ciais P, Dalmonech D, Fisher JB, Fisher RA et al. 2012. A framework of benchmarking land models. *Biogeosciences* **9**: 3857 3874.

Mackay DS, Ahl DE, Ewers BE, Samanta S, Gower ST, Burrows SN. 2003. Physiological tradeoffs in the parameterization of a model of canopy transpiration. *Advances in Water Resources* **26**: 179 194.

Mackay DS, Ewers BE, Loranty MM, Kruger EL, Samanta S. 2012. Bayesian analysis of canopy transpiration models: a test of posterior parameter means against measurements. *Journal of Hydrology* **432□433**: 75 83.

Magori K, Legros M, Puente ME, Focks DA, Scott TW, Lloyd AL, Gould F. 2009. Skeeter buster: a stochastic, spatially explicit modeling tool for studying *Aedes aegypti* population replacement and population suppression strategies. *PLOS Neglected Tropical Diseases* **3**: e508.

Maherali H, Pockman WT, Jackson RB. 2004. Adaptive variation in the vulnerability of woody plants to xylem cavitation. *Ecology* **85**: 2184 2199.

van Mantgem PJ, Stephenson NL, Byrne JC, Daniels LD, Franklin JF, Fulé PZ, Harmon ME, Larson AJ, Smith JM, Taylor AH et al. 2009. Widespread increase of tree mortality rates in the Western United States. *Science* **323**: 521 524.

Marsaglia G, Tsang WW, Wang J. 2003. Evaluating Kolmogorov's distribution. *Journal of Statistical Software* **8**: 1 4.

Marshall JD, Waring RH. 1985. Predicting fine root production and turnover by monitoring root starch and soil tempterature. *Canadian Journal of Forest Research* **15**: 791 800.

Martínez-Vilalta J, Pinol J, Beven K. 2002. A hydraulic model to predict drought-induced mortality in woody plants: an application to climate change in the Mediterranean. *Ecological Modeling* **155**: 127 147.

McDowell NG. 2011. Mechanisms linking drought, hydraulics, carbon metabolism, and vegetation mortality. *Plant Physiology* **155**: 1051 1059.

McDowell NG, Beerling DJ, Breshears DD, Fisher RA, Raffa KF, Stitt M. 2011. The interdependence of mechanisms underlying climate-driven vegetation mortality. *Trends in Ecology and Evolution* **26**: 523 532.

McDowell NG, Pockman W, Allen C, Breshears D, Cobb N, Kolb T, Plaut J, Sperry J, West A, Williams D et al. 2008. Mechanisms of plant survival and mortality during drought: why do some plants survive while others succumb? *New Phytologist* **178**: 719 739.

McDowell NG, Sevanto S. 2010. The mechanisms of carbon starvation: how, when, or does it even occur at all? *New Phytologist* **186**: 264 266.

Meddens AJH, Hicke JA, Ferguson CA. 2012. Spatiotemporal patterns of observed bark beetle caused tree mortality in British Columbia and the western United States. *Ecological Applications* **22**: 1876–1891.

Medvigy D, Moorcroft PR. 2012. Predicting ecosystem dynamics at regional scales: an evaluation of a terrestrial biosphere model for the forests of northeastern North America. *Philosophical Transactions of the Royal Society of London. Series B, Biological sciences* **367**: 222–235.

Medvigy D, Wofsy SC, Munger JW, Hollinger DY, Moorcroft PR. 2009. Mechanistic scaling of ecosystem function and dynamics in space and time: Ecosystem Demography model version 2. *Journal of Geophysical Research* **114**: G01002.

Mitchell PJ, O'Grady AP, Tissue DT, White DA, Ottenschlaeger ML, Pinkard EA. 2013. Drought response strategies define the relative contributions of hydraulic dysfunction and carbohydrate depletion during tree mortality. *New Phytologist* **197**: 862–872.

Moorcroft PR. 2006. How close are we to a predictive science of the biosphere? *Trends in Ecology and Evolution* **21**: 400–407.

Moorcroft PR, Hurtt GC, Pacala SW. 2001. A method for scaling vegetation dynamics: the ecosystem demography model (ED). *Ecological Monographs* **71**: 557–585.

Mu Q, Zhao M, Kimball J, McDowell N, Running S. 2013. A remote sensed global terrestrial drought severity index. *Bulletin of the American Meteorological Society* **94**: 83–98.

Mueller B, Pantin F, Génard M, Turc O, Freixes S, Piques M, Gibon Y. 2011. Water deficits uncouple growth from photosynthesis, increase C content, and modify the relationship between C and growth in sink organs. *Journal of Experimental Botany* **62**: 1715–1729.

Ogée J, Brunet Y, Loustau D, Berbigier P, Delzon S. 2003. MuSICA, a CO_2, water and energy multi-layer, multi-leaf pine forest model: evaluation from hourly to yearly time scales and sensitivity analysis. *Global Change Biology* **9**: 697–717.

Oleson KW, Lawrence DM, Bonan GB, Flanner MG, Kluzek E, Lawrence PJ, Levis S, Swenson SC, Thornton PE, Dai A et al. 2010. *Technical description of version 4.0 of the Community Land Model (CLM). NCAR/TN-478 + STR.* Boulder, CO, USA: National Center for Atmospheric Research.

Pammenter NW, Van der Willigen C. 1998. A mathematical and statistical analysis of the curves illustrating vulnerability of xylem to cavitation. *Tree Physiology* **18**: 589–593.

Pangle RE, Hill JP, Plaut JA, Yepez EA, Elliot JR, Gehres N, McDowell NG, Pockman WT. 2012. Methodology and performance of a rainfall manipulation experiment in piñon–juniper woodland. *Ecosphere* **3**: art28.

Peng S, Ma Z, Lei X, Zhu Q, Chen H, Wang W, Liu S, Li W, Fang X, Zhou X. 2011. A drought-induced pervasive increase in tree mortality across Canada's boreal forest. *Nature Climate Change* **1**: 467–471.

Phillips OL, van der Heijden G, Lewis SL, López-González G, Aragão LEOC, Lloyd J, Malhi Y, Monteagudo A, Almeida S, Dávila EA et al. 2010. Drought–mortality relationships for tropical forests. *New Phytologist* **187**: 631–646.

Plaut J, Wadsworth WD, Pangle R, Yepez EA, McDowell NG, Pockman WT. 2013. Reduced transpiration response to precipitation pulses precedes mortality in a piñon–juniper woodland subject to prolonged drought. *New Phytologist.* **200**: 375–387.

Plaut JA, Yepez EA, Hill J, Pangle R, Sperry JS, Pockman WT, McDowell NG. 2012. Hydraulic limits preceding mortality in a piñon-juniper woodland under experimental drought. *Plant, Cell & Environment* **35**: 1601–1617.

Powell TL, Galbraith DR, Christoffersen BO, Harper A, Imbuzeiro HMA, Rowland L, Almeida S, Brando PM, Lola de Casta AC, Costa MH et al. 2013. Confronting model predictions of carbon fluxes with measurements of Amazon forests subjected to experimental drought. *New Phytologist.* **200**: 350–365.

Purves D, Pacala S. 2008. Predictive models of forest dynamics. *Science* **320**: 1452–1453.

Quirk J, McDowell NG, Leake JR, Hudson PJ, Beerling DJ. 2013. Increased susceptibility to drought-induced mortality in *Sequoia sempervirens* (cupressaceae) trees under cenozoic atmospheric carbon dioxide starvation. *American Journal of Botany* **100**: 582–591.

Raffa KF, Aukema BH, Bentz BJ, Carroll AL, Hicke JA, Turner MG, Romme WH. 2008. Cross-scale drivers of natural disturbances prone to anthropogenic amplification: the dynamics of bark beetle eruptions. *BioScience* **58**: 501–517.

Rasse DP, Tocquin P. 2006. Leaf carbohydrate controls over Arabidopsis growth and response to elevated CO_2: an experimentally based model. *New Phytologist* **173**: 500–513.

Richardson AD, Carbone MS, Keenan TF, Czimczik CI, Hollinger DY, Murakami P, Schaberg PG, Xu X. 2013. Seasonal dynamics and age of stemwood nonstructural carbohydrates in temperate forest trees. *New Phytologist* **197**: 850–861.

Romme WH, Allen CD, Bailey JD, Baker WL, Bestelmeyer BT, Brown PT, Eisenhart KS, Floyd MS, Huffman DW, Jacobs BE et al. 2009. Historical and modern disturbance regimes, stand structures, and landscape dynamics in piñon–juniper vegetation of the western United States. *Rangeland Ecology and Management* **62**: 203–222.

Sala A, Piper F, Hoch G. 2010. Physiological mechanisms of drought-induced tree mortality are far from being resolved. *New Phytologist* **186**: 274–281.

Sala A, Woodruff DR, Meinzer FC. 2012. Carbon dynamics in trees: feast or famine? *Tree Physiology* **32**: 764–775.

Schenk HJ, Jackson RB. 2005. Mapping the global distribution of deep roots in relation to climate and soil characteristics. *Geoderma* **126**: 129–140.

Secchi R, Zwieniecki MA. 2012. Analysis of xylem sap from functional (nonembolized) and nonfunctional (embolized) vessels of *Populus nigra*: chemistry of refilling. *Plant Physiology* **160**: 955–964.

Sevanto S, McDowell NG, Dickman LT, Pangle R, Pockman WT. 2013. How do trees die? A test of the hydraulic failure and carbon starvation hypotheses. *Plant, Cell & Environment.* doi: 10.1111/pce.12141.

Sitch S, Huntingford C, Gedney N, Levy PE, Lomas M, Piao SL, Betts R, Ciais P, Cox P, Friedlingstein P. 2008. Evaluation of the terrestrial carbon cycle, future plant geography and climate-carbon cycle feedbacks using five Dynamic Global Vegetation Models (DGVMs). *Global Change Biology* **14**: 2015–2039.

Sitch S, Smith B, Prentice IC, Arneth A, Bondeau A, Cramer W, Kaplan JO, Levis S, Lucht W, Sykes MT et al. 2003. Evaluation of ecosystem dynamics, plant geography and terrestrial carbon cycling in the LPJ dynamic global vegetation model. *Global Change Biology* **9**: 161–185.

Smith AM, Stitt M. 2007. Coordination of carbon supply and plant growth. *Plant, Cell & Environment* **30**: 1126–1149.

Sperry JS, Adler FR, Campbell GS, Comstock JP. 1998. Limitation of plant water use by rhizosphere and xylem conductance: results from a model. *Plant, Cell & Environment* **21**: 347–359.

Sperry JS, Tyree MT. 1988. Mechansims of water stress-induced xylem embolism. *Plant Physiology* **88**: 581–587.

Stitt M, Zeeman SC. 2012. Starch turnover: pathways, regulation and role in growth. *Current Opinion in Plant Biology* **15**: 282–292.

Sulpice R, Pyl ET, Ishihara H, Trenkamp S, Steinfath M, Witucka-Wall H, Gibon Y, Usadel B, Poree F, Piques MC et al. 2009. Starch as a major integrator in the regulation of plant growth. *Proceedings of the National Academy of Sciences, USA* **106**: 10348–10353.

Thornley JHM. 1972. A model to describe the partitioning of photosynthate during vegetative plant growth. *Annals of Botany* **36**: 419–430.

Tyree MT, Sperry JS. 1988. Do woody plants operate near the point of catastrophic xylem dysfunction caused by dynamic water stress- answers from a model. *Plant Physiology* **88**: 574–580.

Wand MP, Coull BA, French JL, Ganguli B, Kammann EE, Staudenmayer J, Zanobetti A. 2009. *SemiPar 1.0. An R package for semiparametric regression.* [WWW document] URL http://cran.r-project.org/web/packages/SemiPar [accessed 1 July 2013].

Ward JK, Harris JM, Cerling TE, Wiedenhoeft A, Lott MJ, Dearing M-D, Coltrain JB, Ehleringer JR. 2005. Carbon starvation in glacial trees recovered from the La Brea tar pits, southern California. *Proceedings of the National Academy of Sciences, USA* **102**: 690–694.

Waring RH. 1987. Characteristics of trees predisposed to die. *BioScience* **37**: 569–577.

Waring RH, Pitman GB. 1985. Modifying lodgepole pine stands to change susceptibility to mountain pine beetle attack. *Ecology* **66**: 889–897.

Waring RH, Schlesinger WH. 1985. *Forest ecosystems: concepts and management.* Orlando, FL, USA: Academic Press.

West AG, Hultine KR, Sperry JS, Bush SE, Ehleringer JR. 2007. Transpiration and hydraulic strategies in a pinon–juniper woodland. *Ecological Applications* **18**: 911–927.

Wiley E, Helliker B. 2012. A re-evaluation of carbon storage in trees lends to greater support for carbon limitation to growth. *New Phytologist* 195: 285 289.

Williams M, Law BE, Anthoni PM, Unsworth MH. 2001. Use of a simulation model and ecosystem flux data to examine carbon water interactions in ponderosa pine. *Tree Physiology* 21: 287 298.

Williams AP, Allen CD, Macalady AK, Griffin D, Woodhouse CA, Meko DM, Swetnam TW, Rauscher SA, Seager R, Grissino-Mayer HD et al. 2013. Temperature as a potent driver of regional forest drought stress and tree mortality. *Nature Climate Change* 3: 292 297.

Woodward FI, Lomas MR. 2004. Vegetation dynamics-simulating responses to climatic change. *Biological Reviews* 79: 643 670.

Wulder MA, White JC, Bentz B, Alvarez MF, Coops NC. 2006. Estimating the probability of mountain pine beetle red-attack damage. *Remote Sensing of Environment* 101: 150 166.

Xu C, Fisher R, Wilson C, Wullschleger S, McDowell NG. 2012. Toward a mechanistic modeling of nitrogen limitation on vegetation dynamics. *PLoS ONE* 7: e37914.

Zaehle S, Friend AD, Friedlingstein P, Dentener F, Peylin P, Schulz M. 2010. Carbon and nitrogen cycle dynamics in the O-CN land surface model: role of the nitrogen cycle in the historical terrestrial carbon balance. *Global Biogeochemical Cycles* 24: GB1006.

Zwieniecki MA, Holbrook NM. 2009. Confronting Maxwell's demon: biophysics of xylem embolism repair. *Trends in Plant Sciences* 14: 530 534.

Supporting Information

Additional supporting information may be found in the online version of this article.

Fig. S1 MuSICA model simulations of PLC in piñon pine using different vulnerability curves to predict loss of xylem conductivity with decreasing xylem water potential.

Fig. S2 Modeled versus measured predawn leaf water potential via the Sperry model.

Fig. S3 Example of the prediction of soil water potential using ED (X) for an ambient plot at 15 cm soil depth.

Table S1 A summary of how empirical variables were utilized or simulated by models.

Notes S1 Vulnerability to Cavitation.

Notes S2 (a) Estimates of maintenance respiration and allometric calculations. (b) Measurement of non-structural carbohydrates (NSC).

Notes S3 Model-specific developments and application.

Notes S4 On growth efficiency as a predictor of mortality.

Notes S5 Additional References cited in the Supplemental Information.

Please note: Wiley-Blackwell are not responsible for the content or functionality of any supporting information supplied by the authors. Any queries (other than missing material) should be directed to the *New Phytologist* Central Office.